修 士 学 位 論 文

Tolerance of Fe(II) Toxicity by Cyanobacteria Inhabiting an Iron-rich Hot Spring

鉄含有温泉に生息するシアノバクテリアの鉄毒性に対する耐性（英文）

指導教員　　松浦　克美　　教授

平成　30　年　　1　月　　10　日　　提出

首都大学東京大学院

理工学研究科　　生命科学専攻

学修番号　16881303

氏　名　出井愛理

Contents

1. Abstract ..... - 1 -

2. Acknowledgments ..... - 3 -

3. Introduction ..... - 4 -

4. Materials and Methods ..... - 7 -

5. Results ..... - 13 -

6. Discussion ..... - 22 -

7. References ..... - 24 -

8. Tables and Figures ..... - 27 -

1. Abstract

Microbial metabolism in iron-rich hot springs can provide insights into the role of both ancient and contemporary microbes related to iron oxidation. The oxidation of Fe(II) in some ancient periods, resulting in iron deposition, can partially be understood from the reaction with oxygen produced by cyanobacteria or oxygenic phototrophs. However, Fe(II) together with oxygen is toxic to many organisms, and cyanobacteria are no exception. A previous study showed that cyanobacteria responded negatively to anoxic and Fe(II) rich conditions. In this study, cyanobacteria obtained from iron-rich environments were tested to determine whether they were tolerant to iron-rich conditions.

Two types of enrichment culture were obtained from microbial mats in Jinata hot springs in Shikine island, one of Izu islands. The marine hot springs had neutral pH and included 250 μM Fe(II). One area contained unicellular cyanobacteria (JNT 01) and phylogenetic analysis indicated that the bacterium is related to *Cyanobacterium aponium* (99 % identity).

Cyanobacteria from the springs were cultured in the absence of Fe(II), aerobically. Then, the cyanobacteria cultured were grown in air-tight bottles under anoxic and Fe(II) containing conditions, at the beginning, in order to reveal the effect of Fe(II) on growth. The growth of one microcosm, containing a morphotype referred to here as JNT 01, was different from *Synechococcus* PCC 7002, as a control. JNT 01 in 600 μM initial Fe(II) grew as fast as in 0 μM Fe(II). The growth of *Synechococcus* PCC 7002 in 600 μM Fe(II) was about half of the growth in 0 μM Fe(II). During the growth of cells, the Fe(II) concentration diminished in several hours in both cultures. To reveal the difference in the growth of JNT 01 and *Synechococcus* PCC 7002 with Fe(II) in early growth phase, the growth conditions were changed. *Synechococcus* PCC 7002 sometimes grew in 200 μM better than in 0 μM. It seems to be the effect of Fe on the metabolism.

Therefore, the timing of the addition of ferric citrate – a growth nutrient – was changed from before autoclaving to after autoclaving. Under the changed conditions, the growth of JNT 01 and *Synechococcus* PCC 7002 was similar. These experiments seemed to suggest that *Synechococcus* PCC 7002, but not JNT 01, was sensitive to an effect of the form of Fe as a nutrient for growth, and that the timing of autoclaving affected this.

Since Fe(II) decreased in less than 24 hours in these experiments, it was difficult to make conclusions about the effects of Fe(II). To investigate these effects on growing cells, the initial growth of cells was examined. Less than 24 hours after the start of growth, Fe(II) was decreasing but still present. During this period, the growth of JNT 01 is significantly different from the growth of PCC 7002. In the later time when Fe(II) decreased, the difference became less significant.

These results together suggested that the enriched unicellular cyanobacteria inhabiting in the Fe(II)-rich hot springs were tolerant to the ferrous iron rich conditions. It is possible that they have been adapted to iron-rich environments which are similar to that expected for Precambrian environments. This study provides insights into ancient iron transformations and mechanisms of Fe(II) toxicity in both modern and ancient ocean cyanobacteria.

2. Acknowledgments

I would like to express my gratitude to everyone who has helped me throughout my graduate study. First and foremost, I would like to thank the main supervisor, Dr. Shawn McGlynn for his generous support, guidance, and warm encouragement throughout my undergraduate and graduate studies. We discussed every week despite the distance even after he has moved out from Tokyo Metropolitan University. I would like to thank my supervisor, Dr. Katsumi Matsuura, for his enormous support and affectionate education throughout my studies and laboratory life. I am deeply grateful to Dr. Shin Haruta for his valuable advice and suggestion.

I want to thank Dr. Sigeki Ehira for the insightful advice and help of the experiments. I appreciate the support by Drs. Satoshi Hanada, Vera Thiel, and Marcus Tank for their constructive comments and great interests. Finally, I would like to offer my special thanks to Environmental Microbiology laboratory members for their support and encouragement throughout this study and my research life.

3. Introduction

The physiology and ecology of microbes in iron-rich environments have been the focus of extensive studies for understanding ancient and contemporary interactions between Fe ions and microbial communities. Before the Great Oxidation Event between 2.4 and 2.3 billion years ago (Bekker et al., 2004; Claire et al., 2006; Farquhar et al., 2011; Lyons et al., 2014), Precambrian springs, rivers, lakes and oceans were anoxic and rich with Fe(II) ions (Canfield, 1998; Planavsky et al., 2011; Poulton and Canfield, 2011). Dissolved Fe(II) concentrations in the ancient ocean are estimated to be between 40 and 120 μM (Holland, 2003; Kappler et al., 2005). Dissolved ferrous irons changed to ferric irons in the during earth's history, and ferric irons precipitated as ferrihydrite and then resulted in iron mineral formations, so called Banded Iron Formations (BIFs). The process of BIF deposition has been discussed and studied extensively (e.g. Anbar et al., 2007), and this great change is thought to be tightly connected to the evolution of cyanobacteria or early oxygenic phototrophs in the Precambrian through the oxidation of the atmosphere, hydrosphere, and lithosphere (Cairns-Smith, 1978; Cloud, 1968; Kappler et al., 2005; Konhauser et al., 2002; Trouwborst et al., 2007). Most Fe(II) in the ocean had probably deposited by around 2 billion years ago, and thereafter the increase in the atmospheric oxygen content became more significant (Tangalos et al., 2010).

Fe(II) plus oxygen is toxic to many organisms, and cyanobacteria are known to be affected by Fe(II) and oxygen emitted from themselves. Although various heavy metal ions are essential for various metabolic processes in organisms in trace amounts, they can induce physiological stress leading to the generation of free radicals in high concentration (Choudhary et al., 2007; Debelius et al., 2009; Rai et al., 1981; Swanner et al., 2015). Previous studies have demonstrated that the relationship among cyanobacteria, Fe (II), and photosynthetic oxygen

production is influenced by the production of reactive oxygen species (ROS) when oxygen reacts with Fe(II) (Raiet al. 1981; Debelius et al. 2009; Swanner et al., 2015). Fe (II) toxicity was related to enhanced intracellular concentrations of ROS, which results in a decrease in the efficiency of oxygenic photosynthesis, possibly due to the inhibited repair of damaged photosystems and the decreased growth rate (Swanner et al., 2015).

Archean oceans contained significantly more Fe (II) than contemporary environments (Barbeau et al., 2001; Brown et al., 2005; Pierson et al., 1999), because dissolved ferrous irons in current oxygenic environments rapidly oxidizes to ferric irons. In iron rich environments, iron detoxification mechanisms would have been necessary for cellular survival especially as oxygen was introduced into the atmosphere. The survival process of microbe coexistence with iron and oxygen is still mysterious, but a few previous studies have tested how cyanobacteria respond to anoxic and Fe(II) rich conditions (Rantamäki et al., 2016; Swanner et al., 2015). In these studies, photosynthetic reactions under anaerobic conditions were examined in *Synechococcus* PCC 7002, *Nodularia spumigena*, and *Microcystis aeruginosa* with high Fe(II) concentrations to infer the Fe (II) toxicity. Furthermore, in a microbial ecological review of neutral pH springs with Fe(II) ions, cyanobacteria were present in springs with less than 80 μM Fe (II) in the source waters or within the microbial mats (Swanner et al., 2015). Although the iron-dependent physiology of marine and fresh-water cyanobacteria has been the focus of some study (Achilles et al., 2003; Barbeau et al., 2001; Michel and Pistorius, 2004), the physiology and diversity of cyanobacteria inhabiting iron rich hot springs and waters have not been studied in detail, as well as possible relationships of those cyanobacteria to ancient, microbial iron transformations.

As one of the ideal research sites, Jinata hot spring in Shikine island, one of Izu islands in Tokyo prefecture in Japan, contains about 200 μM ferrous irons at the source water at pH 5.4 and about 63 °C. There are 4 pools, which are connected by channels and flown out to the ocean at

the end. A colorful ferric iron formation is being deposited in these hot springs. The soft sediments were orange-ish probably due to oxidized iron. Phototrophic mats were formed by cyanobacteria at the interface of the iron sediments and water in three pools. In addition, small colonies of unicellular cyanobacteria were found under the orange mineral layer. These microbial mats mainly composed of cyanobacteria may play a substantial role in the formation of the iron oxide, thereby promoting the accumulation of a soft precipitate that can be compressed to form iron precipitate.

In this study, cyanobacteria obtained from the Fe(II) rich spring water at Jinata hot spring, were tested whether they were tolerant to the iron-rich conditions. The growth experiments were designed to give an idea on how much iron could be tolerated by the cyanobacteria. Physiological experiments were conducted to investigate the tolerance of the Fe (II) to toxicity by cyanobacteria. The diversity and physiological study of cyanobacteria in iron rich environments can give insights how they survive in modern and ancient iron rich environments.

4. Materials and Methods

Information of sampling site

Jinata hot spring is located at approximately 13’12’57” E; 34’19’5” N on the Shikine-island, Tokyo Prefecture in Japan (Fig. 1 a-b). Shikine-island is one of the Izu-islands, a chain of volcanic islands, which formed in last few million years along the northern edge of the Izu-Bonin-Mariana Arc (Hirata et al., 2010). The source water of Jinata hot spring was nearly anoxic iron rich and bubbling CO_2 from the source. The salt concentration was 4 % and similar to sea water. Temperatures at the source were ~66 °C. Hot spring water emerged into the Pool 1 and didn’t mix with sea water in the pool. Surfaces of the bottom are covered with fluffy orange-ish deposits, likely a poorly-ordered iron oxide phase such as ferrihydrite. Microbial mats or biofilms were not observed in the source pool, but some easily broken streamers were. Downstream of the Pool 1, the spring water flowed into a series of pools (Pool 2-4), which the temperature of pools gradually cooled down (Fig. 1 c). The bottom of Pool 2 is dominated by precipitated iron deposits, like Pool 1. There were green microbial mats at the surface of the deep part about 30cm depth of Pool 2. An outlet of a channel connected Pool 2 to the ocean and also to Pool 3. The bottom of Pool 3 and 4 are covered with thick microbial mats with small babbles (Fig. 1 l) in the surface of the mats. In Pool 4, the water flowed constantly to the ocean and mixed with sea water.

Sample collection

Samples were taken on September 14th -15th in 2016 at Jinata hot spring. The high tide was 145 cm at 16:33 on 14th. The low tide was 27cm at 10:30 on 15th. At low tide, the source water stopped flowing and the pool was dry with exception of a few standing puddles. The samples were collected at the high tide. Samples of water, orange sediments and microbial mats were collected

from five sites in Pool 1-4. Site 1 was close to the source of spring water at the deep part in Pool 1 (Fig. 1 h). The depth was about 50 cm at the highest tide. Site2 in the downstream part of Pool 1 contained streamers at the bottom (Fig. 1 i), which were easily broken by a touch. At site 3 and 4, the deposits consisted of 3 layers. The top was a green mat (thickness was about 1mm). The second was an orange layer. The bottom was a black layer (Fig. 1 j, k). The samples were collected from each layer. Site 5 contained green mats and oxygen bubbles on the top of them in Pool 4 (Fig. 1 l).

Geochemical analysis

Dissolved oxygen (DO), pH, and temperature, and salinity measurements were performed in situ using an Extech DO700 8-in-1 Portable Dissolved Oxygen Meter. The gas content was previously measured (McGlynn unpublished).

Media and cultivation

Immediately after collection, cyanobacterial mats with fluffy sediments, and black sediments samples were immersed in 50 ml tubes containing the water at the site. The samples were cultivated under static conditions on ASN-III medium in Erlenmeyer flasks with paper stopper at 45 °C under an irradiance of about 20 μmol photonsm^{-1} s^{-1} from standard fluorescent lights. ASN-III medium contained (per liter) 25 g NaCl, 2.0 g $MgCl_2$, 0.5 g KCl, 0.75 g $NaNO_3$, 20 mg K_2HPO_4, 3.5 g $MgSO_4$, 0.5 g $CaCl_2$, 20 mg Na_2CO_3, 1 ml Trace metal mix5A+Co, 1 ml of stock solution 1 and 20 ml of 1M Hepes. Trace metal mix 5A+Co (100 ml) contains 286 mg boric acid, 181 mg manganous choloride tetrahydrte, 22.2 mg zinc sulfate heptahydrate, 39 mg sodium molybdate dihydrate, 7.9 mg copper sulfate pentahydrate, 4.9 mg cobalt (II) nitrate hexahydrate. Stock solution1 (100 ml) contains 0.3 g citric acid, 0.3 g ferric ammonium citrate and 0.5 g Na_2EDTA.

The pH was adjusted to 7.5 with KOH. As a control, an axenic culture of *Synechococcu*s PCC 7002 was used. It was cultivated under static conditions on ASN-III medium at 30 °C and pH 7.5.

Analysis methods

Growth was measured by monitoring the increase in chlorophyll (Chl) concentration. In each time of measurement, cells of aliquots (1 ml) of cultures were collected (12,000 rpm, 5 min). 950 µl of the supernatant was removed. The pellets were mixed and incubated overnight in methanol (950 µl) in the dark, and absorbance was measured at 665 nm and 750 nm with photo spectrometer (UV-1800, SHIMADZU) for the cultures. In the experiments of the small amount of cells (Chl: 0.05 µg/ml), Chl was detected with the multimode plate reader (Infinite® M200 PRO, TECAN) by 96 wells. Chl concentrations were calculated from the equation Chl (µg/ ml) = 13.49 × (A_{665}–A_{750}) (Rantamäki et al., 2016). For JNT 02, the filamentous cyanobacteria, the biofilms formed on the surface of test tubes were broken by glass beads with the diameter of 3 mm. For determining the approximate cell density with the turbidity for dilution or concentration, optical density was measured at 750 nm.

Ferrous iron contents were measured by using the ferrozine assay (Stookey, 1970). The solutions for ferrozine assay were the ferrozine solution and acetate buffer. The ferrozine solution (1.225 mM, 100 ml total) was mixture of 0.06253 g Ferrozine and 50 µl of 2 M HCl. The acetate buffer was 6.87 M, 100 ml total. 30 ml of water was added 34.95 g sodium acetate anhydrous slightly to get into solution while keeping warm. It was added 15 ml of glacial acetic acid and brought to 100 ml. Aliquots (0.5 ml) of cultures were added to 0.5 ml of 0.2 M HCl in order to keep ferrous concentration. Fe (II) was measured with ferrozine solution in an acetate buffer at 526 nm on the spectrophotometer. The volume of a sample was 600 µl. The volume of ferrozine solution was 160 µl. The volume of acetate buffer was 200 µl. The volume of water was 40 µl.

Molecular methods (16S rRNA gene sequencing)

Genomic DNA was extracted from field environmental samples and enrichment cultures. They were collected in 2.0 ml screw capped (bead beating tubes) tubes. The cell pellets (8,000 rpm, 5 min) were added 700 µl of TPE buffer with zilconia-silica beads. TPE buffer contained 50 mM Tris-HCl (pH 7.0), 1.7 % (wt/vol) polyvinyl pyrrolidon K25 and 20 mM $MgCl_2$. The mixtures were beaten and centrifuged (11,000 rpm, 5 min, 4 °C). The supernatant was collected and added 10% CTAB (Hexadecyltrimethylammonium Bromide). The solutions were incubated for 20 min at 60 °C (Noll et al., 2005) and 100 µl of 5 M NaCl. The supernatants were added 600 µl of CIA. CIA was Chloroform and isoamyl alcohol (24:1). The solutions were mixed by a vortex mixer and centrifuged (15,000 rpm, 5min). The supernatants were collected in new tube and added 600 µl of PCI. PCI contained Phenol, Chloroform and Isoamyl alcohol（25:24:1）. The solutions were mixed by a vortex mixer and centrifuged (15,000 rpm, 5 min). The supernatants were collected in new tubes collected and added 55 µl of 3 M NaOAC and 600 µl of isopropanol. The solutions were centrifuged (15,000 rpm, 10 min) and removed the supernatants by an aspirator. The pellets were added 600 µl of 70 % EtOH and centrifuged (15,000 rpm, 5 min). The supernatants were removed by an aspirator and added 30 µl of TE buffer and kept in a freezer (-20 °C). TE buffer contained 10 mM Tris-HCl and 1 mM EDTA (pH 8.0).

PCR mediated amplification of genomic DNA was performed using universal primers and cyanobacteria 16S rRNA gene-specific primers. For the unicellular cyanobacteria in enrichment culture, primers 27F, 907R and 1427R were used. For filamentous cyanobacteria, the specific cyanobacterial primers were used (Table 2 Primer sets). The PCR product was sequenced, and the resulting sequences were analyzed by BLAST against 16S rRNA sequences from Gene Bank (Gen Bank database of the National Center for Biotechnology Information,

http://www.ncbi.nlm.nih.gov/)

Light microscopy

Light microscopy images were taken with Zeiss Axio Imagers 2 Upright microscope (Zeiss, Germany) with 40 x (Zeiss Plan-NEOFLUAR) and 100 x (Zeiss Plan-APOCHROMAT) objective lens. Samples were incubated with 4 % formaldehyde final concentrations in PBS (pH 6.9) for 1 hours to fix cells. After fixing, samples were washed by 50mM Hepes (pH 7.6) three times by pelleting and re-suspending the cells by centrifugation (12,000 rpm, 3 min). They were stained by a solution of 1 µg/ml DAPI (4',6-diamidino-2-phenylindole) on slides. Fluorescent images of DAPI -stained samples were taken with an excitation wavelength below 395 nm and an emission wavelength between 420 nm and 470 nm. The auto fluorescence of cyanobacteria was detected by exposing the sample to excitation light with wavelengths of between 395 nm and 440 nm and the emission of over 470 nm. Images of DAPI fluorescence and auto fluorescence were overlaid using the FIJI software package (http://pacific.mpi-cbg.de).

Scanning electron microscopy and Energy Dispersive X-ray Spectrometry

For SEM, the samples were put on the conductive ITO coated glass and dried in air. Sample mounts were visualized using a JEOL JSM-6100 SEM, with a LaB6 source and a Hummer VII coating device (Anatech Ltd). Elemental analysis was detected using EDS - Quantax with Silicon Drift Detector (SDD) X Flash (BRUKER123eV).

Cultivation under iron rich conditions

In the growth experiments of unicellular cyanobacteria, cells were grown in 120 ml glass bottles with butyl rubber stoppers. 28 ml or 28.9 ml of ASN-III medium in the bottles were degassed by

N_2 for 20 minutes to make anaerobic conditions. Then, the gas phase was exchanged with N_2/CO_2 (80:20 v/v). Fe(II) was added as a filter-sterilized $FeCl_2$ stock solution in an anaerobic ASN-III medium, pH 4. Additions of 1 ml of 6 mM, 18 mM and 30 mM Fe(II) stock solutions resulted in the Fe (II) concentrations 200 μM, 600 μM, 1000 μM in culture bottles. Before inoculating cyanobacteria, the bottles were kept in the dark for overnight. Cyanobacterial cells for inoculation were collected from a pre-culture incubated for 5-7 days and washed by the medium anaerobically. For the comparison between JNT 01 and *Synechococcu*s PCC 7002, the amounts of cells of inoculation was adjusted to be the same by measuring Chl concentrations. In the growth experiments, two initial concentrations, 0.5 μg/ml chlorophyll conditions and 0.05 μg/ml chlorophyll conditions were used. Inoculations were made by inoculating the cells appropriate amounts of cells into the anoxic, Fe(II)-containing medium. In the growth experiments of filamentous cyanobacteria, the filamentous cells were grown in 30 ml test tubes with rubber stoppers. The anaerobic medium containing Fe (II) concentrations were made as for the unicellular experiments.

For experiments testing effects of Fe(III), 0.4 M Ferrihydrite stock were prepared. 5.4 g $FeCl_3 \cdot 6H_2O$ were added to 50 mL water. 1N NaOH was dropped into the solution with stirring until pH changed to 7. The color was changed from transparent to black brown to turbid red brown around pH 6 - 7. Total volume of dropped NaOH was about 50ml. The ferrihydrite solution was centrifuged (5,000 rpm, 10 min).The ferrihydrite particles were collected and washed by 50 mM Hepes (pH 7.6) three times.

Calculation of Growth rate

Growth rate were calculated by $dN/dt = kN$. N is the concentration of Chl, t is the time and μ is the growth rate. The specific growth rate μ is calculated by: $\mu = ln (N2 / N1) / (t2 - t1)$.

5. Results

Water chemistry of Jinata hot springs

Source waters were slightly enriched in sodium chloride relative to seawater. The temperature of water emerging from the source was 65 °C and had of pH 5.4 (Table 1). It contained significant amounts of dissolved iron (~200 μM Fe(II)). Seawater is slightly mixed in Pools 2 and 3, and significantly mixed in Pool 4 although the mixed ratio was depended in the tides. After emerging from Pool 1, the spring water exchanged gases more intensely with the air due to mixing by turbulent water flow between pools and gas bubbling at the flow. As water flows downstream from the source pool, it cooled slightly below Pool 2. The oxygen from the atmosphere was mixed in but Fe (II) remained at high concentration. In Pool 4 the Fe (II) concentration decreased half compere to the source water, probably because of mixing with seawater.

Observation of microbial mats and cells

Microbial mats and sediments samples from the hot springs were observed to know the presence of microbes, especially cyanobacteria, using fluorescence microscopy. In all samples from five sites, the presence of cells was observed. At Site 1 and Site 2 of Pool 1, there were associated microbes with orange particles (Fig. 2 a, b). At those sites, no green mats and cyanobacteria were observed. At Sites 3 and 4, black color layers were observed under a green mat. The black layers contained unicellular cyanobacteria (Fig. 2 c, d). The size of the spherical unicellular cyanobacteria was 2.5-4 μm in diameter. In the microbial mats, filamentous cyanobacteria were observed with a straight filamentous shape without branching (Fig. 2 e, f). The cells with the same morphology were aggregated. Microbial green mats from Site 3, 4, 5 were dominated by similar filamentous cyanobacteria.

Observation of unicellular cyanobacteria using Scanning Electron Microscopy

In order to identify chemical compounds in mineral particles associated with cyanobacteria, pictures of microscopy and SEM were merged and compared to SEM-EDS image. The merged image of fluorescence microscopy and light microscopy (Fig. 3 a) shows the position of what are likely unicellular cyanobacteria in orange color. The EDS image (Fig. 3 e) was part of the same field in Figure 3 a-c, focusing on cyanobacteria. It indicates the position of Fe (blue) and C (red) in mineral particles. The position of C corresponds to cyanobacteria as shown is Fig 3 a. The mineral particles containing Fe covered and stuck on cyanobacteria.

Chemical compositions of sediments

The mineral compositions of three sediments from Sites 1, 3, 5 were measured by SEM-EDS. The sediments of Site 1 and 2 were orange. Site 3 and 4 contained black sediments and orange sediments. Averages atomic compositions of them were C 4-16 %, O 51-62 %, Mg 0.24-1 %, Si 2-6 %, Fe 16-19 % (Fig. 4 d). The orange sediments with mats contained less Mg and Si and the black layer contained 5 % Mn. The black color seems to be due to MnO_2.

Cyanobacteria enrichment cultures

Two types of the enrichment cultures of cyanobacteria were obtained from the sediments and mats. One of them contained unicellular cyanobacteria (JNT 01) obtained from the black layer of Site 3. The other was filamentous cyanobacteria from the green mats of Site 5. By light microscopy, the cells of JNT 01 were pale blue-green, 3-4 μm in diameter, with a mucilaginous sheath (Fig. 5 a). They were solitary and showed a symmetrical division. The filaments of the enrichment culture of JNT 02 were variously curved, flexuous, twisted and entangled (Fig. 5 c). In older liquid

cultures, the mat-like structures were formed on the glass surface, detached from the surface, and became large aggregates. A cell in a filament was 3-6 μm long and 2.5-3.5 μm wide.

The enrichment culture of JNT 01 contains a few kinds of contaminated cells in addition to cyanobacteria. The number of them was around half of JNT01 when they reached full growth. The size of cells was about 1μm. JNT 01 is about 3 μM. According to a calculation from the size, the volume of the contaminated cells was estimated to be occupied about 2 % of the total volume of cells.

Phylogenetic analyses

The seaquencing of the amplified 16S rRNA gene indicated that JNT 01 is related to *Cyanobacterium aponinum* PCC 10605 with a sequence identify of 99 % (Table 3). That organism was isolated from thermal spring in Italy and is a unicellular cyanobacteria that reproduce by transverse binary fission. Cells of the genus are spherical to rod-shaped, 1.7 - 2.3 μm in diameter. In a study, the information of PCC 10605 was not written in detail. Therefore, other strains were referred to. *Cyanobacterium aponinum* ETS-03 and *Cyanobacterium* sp. MBIC 10216 are also clustered with JNT 01 (identify of 99 %). *Cyanobacterium aponinum* ETS-03 (Moro et al., 2007) was isolated from the maturation mud tanks of the Garden Hotel (Padua, Italy). The temperature of the water in the tanks was about 40 °C with pH of 6.8. Cultures were maintained in a growth chamber at 30 °C. *Cyanobacterium* sp. MBIC 10216 was isolated from Sakamoto marine hot spring (Iou Island, Kagoshima, Japan). *Cyanobacterium aponinum* EST-03 survived at temperatures up to 45 °C, while MBIC 10216 did not live above 40 °C. JNT 01 was grown at 45 °C in this study. The filamentous cyanobacteria (JNT 02) was found to be related to *Geitlerinema* sp. BBD P2b-1 with the identify of 99 % (Table 3). This genus differs from *Leptolyngbya* by very active gliding motility and lack of sheath envelopes (Boone and Castenholz,

2012). They may be distinguished from Osillatoria by cell shape (longer than broad) and with some exceptions. *Geitlerinema* sp. BBD P2b-1was isolated from black band disease (BBD) found on tropical coral reefs. *Geitlerinema* sp. BBD P2b-1 is a pathogenic microbial consortium dominated in terms of biomass by phycoerythrin-rich, gliding, filamentous cyanobacteria. This strain characteristics are: motile (gliding), nonheterocystous, unbranched trichomes, 3.0 to 3.9 mm wide, with an average cell length of 2.5–4.0 mm. This strain was cultivated in room temperature, 27 °C (Myers et al., 2007). JNT 02 was grown at 45 °C.

Growth of JNT 01 and Synechococcus PCC 7002 under high Fe (II) concentrations

In order to test the effect of Fe(II), the growth of JNT 01 and *Synechococcus* PCC 7002 was examined in air tight bottles with initial anaerobic conditions. For the Fe (II) concentrations, 200 µM, 600 µM, 1000 µM initial Fe(II) were used. Initial chlorophyll concentrations were adjusted to 0.5 µg/ml. In these experiments, cultures with Fe(II) turned yellow in several hours likely because of Fe(III) particles. After a few days, cultures with 200 µM Fe(II) turned green because of the significant growth of cyanobacteria. But in cultures with higher concentrations of Fe(II), the cultures changed to orange, and Fe(III) particles was deposited (Fig. 6).

The growth of JNT1 in 200 µM and 600 µM initial Fe(II) was as fast as the growth in 0 µM (Fig. 7). Cultures without Fe(II) became slower after 72 hours. The growth of *Synechococcus* PCC 7002 as a control in 600 µM Fe(II) was slower than the growth in 0 µM, although with 200 µM Fe(II) the growth was not different from that in 0 µM. JNT 01 reached full growth after 150 hours but *Synechococcus* PCC 7002 took about 300 hours (Fig. 7 c, f). Fe(II) measurements indicated that Fe(II) concentrations of JNT 01 cultures diminished in 12 hours and that of *Synechococcus* PCC 7002 decreased in 48 hours (Fig. 7 g, h). In the second experiments under the same conditions, JNT 01 showed similar growth of cultures in 200 µM Fe (II) as in 0 µM

Fe(II) for 100 hours (Fig. 8 c). But the cultures with 600 µM Fe(II) were slower at 48hours. The growth of cultures with 1000 µM Fe(II) grew as fast as that with 600 µM Fe(II) at 48 hours. In cultures of *Synechococcus* PCC 7002, the growth curves differed from the first experiment. Between 50 and 120 hours, the cultures with 200 µM Fe (II) grew faster than 0, 600, 1000 µM Fe (II). The concentrations of chlorophyll in cultures with 200 µM Fe (II) were also significantly higher than those in the other three conditions in the same period in the previous experiment during the same period of 50 to 120 hours (Fig. 7 d).

Effects of the addition of Fe(III) particles on growth of JNT 01 and Synechococcus PCC 7002

During the growth of cells, Fe(II) changed to iron oxide particles in several hours and the Fe(II) concentrations decreased, however the effects of different initial concentration of Fe(II) continued. Therefore, the effects of the addition of Fe(III)-particles were examined. The addition of particles with various amounts did not affect the growth of JNT 01 and *Synechococcus* PCC 7002 (Fig. 9). The 1000µM curves of JNT are somewhat lower. But the differences were less than the experiment of Fe(II), and overall there was not a clear relationship between increased iron and growth rate.

Inoculation of small amounts of cells

To reveal the difference between the growth of JNT 01 and *Synechococcus* PCC 7002 with Fe(II) early growth phases before Fe (II) disappeared, the inoculation size was decreased because photosynthetically evolved oxygen was thought to be the cause of the Fe(II) decrease. The initial concentrations of chlorophyll were changed from 0.5 µg/ml to 0.05 µg/ml to make the speeds of Fe (II) oxidation slower (Fig. 10 g, h). In these experiments, 600 µM Fe (II) in cultures of JNT 01 diminished in 24 hours. In 1000 µM Fe(II), the diminishing time decreased from 6 - 12 hours in previous experiments with higher cell densities to 24 - 48 hours. Under the low cell inoculum

conditions JNT 01 with 200 μM Fe(II) grew as fast as 0 μM (Fig. 10). 600 μM Fe (II) affected the growth of the culture for 96 hours; one tube recovered but the other's growth remained depressed. PCC 7002 did not grow well for 80 hours. Between 80 and 120 hours, PCC 7002 with 200 μM Fe (II) grew slowly, but did not grow at 600 μM and 1000 μM Fe(II). After 120 hours there was variation in the levels of full growth (Fig. 10). JNT 01 constantly grew with this small inoculation, but PCC 7002 did not grow constantly with the small inoculation.

Inoculation of small amounts of cells under the conditions of changed ferric citrate addition

In the results of growth experiments with small inoculations, *Synechococcus* PCC 7002 did not grow well (compare Fig. 8 d, Fig. 10 d), and *Synechococcus* PCC 7002 with 200 μM Fe(II) sometimes grew better than in 0 μM. One hypothesis accounting for this was that of an effect of Fe utilization for metabolism. Therefore, the conditions of the growth experiments were changed as to how ferric citrate was added for the Fe source. Ferric citrate contained in the medium is necessary to grow for cyanobacteria as growth nutrient in the present medium (Straus NA, 1994). In order to evaluate the effects of ferric citrate on the Fe (II) experiments, ferric citrate was omitted from the culture medium (Fig. 11, 12).

Under the non-additional ferric citrate conditions, the growth of JNT 01 and *Synechococcus* PCC 7002 was different (Fig. 11 a and d, Fig. 12 a and d). JNT 01 with 200 and 600 μM Fe(II) grew better than zero, and the growth with 1000 μM Fe(II) was actually better than zero (Fig. 12). Under 200 μM and 600 μM Fe (II), JNT 01 grew well after 100 hours. PCC 7002 growth was variable, and dramatically lower than previous cultures and also the JNT 01 experiments. PCC 7002 with 200 μM Fe (II) grew. The cultures of *Synechococcus* PCC 7002 with 200 μM and 600 μM Fe (II) grew at only to 1 μg/ml Chl in 300 hours (Fig. 11 d). Under the no ferric citrate conditions, the cultures of *Synechococcus* PCC 7002 with 200 μM Fe (II) grew slightly (Fig. 12 d), but the levels

of full growth were low. PCC 7002 with higher Fe(II) concentrations did not grow significantly. Fe (II) concentrations were not decreased in 50 hours in the cultures of PCC 7002 without ferric citrate while in JNT 01 culture Fe (II) constantly decreased in 24-48 hours.

By adding the ferric citrate after autoclaving, the growth of PCC 7002 became different comparing to the addition before autoclaving (compare Fig. 10 d, Fig. 13 d and Fig. 14 d). The cultures of both cyanobacteria without Fe (II) and with 200 µM Fe (II) grew similarly. The growth of them with 600 µM Fe (II) was slower or similar to the growth with 200 µM Fe (II) depending on the bottles. Both cyanobacteria under 1000 µM Fe(II) grew more slowly (Fig. 13 a and d).

Fe(II) concentrations decreased steadily in every culture (Fig. 13, g and h). Fe(II) concentrations in the cultures of both cyanobacteria with 1000 µM Fe (II) were diminished in about 48 hours. That of 600 µM Fe (II) were disappeared in about 24 hours in both cultures.

Comparison the growth rate while Fe(II) was present

The effects of Fe (II) on the growth rates were compared under conditions before the whole Fe (II) was oxidized (Fig. 13 g, h); i.e., the growth rates of JNT 01 and PCC 7002 were compared when Fe(II) was present.

In the cultures of both cyanobacteria with 600 µM Fe (II), Fe (II) concentration diminished around 24 hours after the inoculation (Fig. 13 g, h). Fe (II) concentration in the cultures with 1000 µM Fe (II) reduced within around 48 hours. The growth in 48 hours in each culture in the presence of Fe(II) were compared with statistical analysis of three experiments.

In 24 hours, the cultures of JNT 01 grew dependent on Fe(II) concentrations (Fig. 13 b). In 48 hours they also grew. In the culture of 1000 µM Fe(II), the growth was a half of the growth of 0 µM. PCC 7002 with 600 µM and 1000 µM Fe(II) did not grow in 24 hours. In 48 hours, the cultures with 600 µM grew slightly dependent on the bottles, and in the cultures with 1000 µM

Fe(II) PCC 7002 did not grow (Fig. 13 e).

The experiments were done again under the same conditions (Fig. 14, Fig. 15). In 24 hours, the cultures of JNT 01 grew dependent on Fe(II) concentrations similarly to Fig. 13. But the cultures with 1000 μM Fe(II) did not grow in 24 hours. In 48 hours, the cultures with 1000 μM Fe(II) grew slightly. PCC 7002 with 600 μM and 1000 μM did not grow in 24 hours (Fig. 14 e). In 48 hours, the cultures with 600 μM grew slightly and the cultures with 1000 μM did not grow (Fig. 14 e). The culture with 0 μM and 200 μM Fe(II) grew in each period. Experimental conditions of Fig. 14 a-c and Fig. 14 d-f were different in pH. The growth with 1000 μM in pH 8.5 was better than that in pH 7.5 (Fig. 14 a, d).

In order to infer significant differences from these results, the growth rates were compared in 48 hours. The growth rate was calculated from the average data of 4 bottles in the two experiments under the same conditions. For the data of JNT 01, Fig. 13c and Fig. 15 c were used. For the data of PCC 7002, Fig.13 f and Fig. 15 f were used. Comparing the growth rates of JNT 01 indicated that the average growth rates with 1000 μM Fe(II) was about a half of that with 0 μM Fe(II) (Fig. 16). The growth was significant difference between 0 μM Fe(II) and 1000 μM Fe(II) according to one way t-test ($p < 0.05$). On the other hands, the average growth rates of PCC 7002 with 1000 μM Fe(II) was about 1/20 of that with 0 μM Fe(II) (Fig. 16). The growth rate was significant difference between 0 μM Fe(II) and 1000 μM Fe(II) according to one way t-test ($p < 0.01$).

Filamentous cyanobacteria (JNT 02) cultivation with high Fe (II) concentration

Since the filamentous cyanobacteria enrichment formed biofilms as described above, test tubes were used to form biofilms on the glass surface of tubes instead of using sealed bottles. Biofilms were formed on the glass of tubes. For 3 days after inoculation, growth was not observed. Some

cultures with 0 μM, 200 μM and 600 μM showed growth after 6 days. When they were kept a long time (13 days), the filamentous cyanobacteria with 0 μM, 200 μM and 600 μM grew well but showed variations in the growth. A few cultures with 1000 μM grew but there were a small amounts of cells (Fig. 17).

6. Discussion

Jinata hot springs at Shikine island contained high concentrations of ferrous ions (Fe(II)) of around, 200 μM with a temperature up to 66 °C. Oxidized iron particles (likely ferrihydrite) were deposited on the bottom of the pools of hot springs. In comparison of springs with Fe(II) ions, cyanobacteria have been reported to be present in springs with less than 80 μM Fe (II) in source waters or within the microbial mats, but not above that value (Swanner et al., 2015). At Jinata hot springs, spherical unicellular cyanobacteria and filamentous cyanobacteria were found in the iron sediments with high Fe (II) concentrations that were more than that in previous studies (Fig. 2). The unicellular cyanobacteria were associated with the iron particles and the filamentous cyanobacteria formed green colored bacterial mats producing bubbles likely comprised of oxygen.

Enrichment cultures of spherical unicellular cyanobacteria and filamentous cyanobacteria were obtained under the temperature of 45 °C in the laboratory. From analysis of the 16S rRNA gene sequences, the unicellular cyanobacteria, JNT 01, showed 99% identity to *Cyanobacterium aponinum* strain PCC 10605. The filamentous cyanobacteria, JNT02, showed 99% identity to *Geilterinema* sp. BBD_P2b-1. All of these reported cyanobacterial strains were isolated from environments without ferrous ions (Moro et al., 2007; Myers et al., 2007). The two cyanobacteria in the enrichment cultures obtained here may have adapted to Fe(II) rich environments.

Effects of high concentrations of Fe(II), from 200 μM Fe(II) to 1000 μM Fe(II) on the growth of JNT 01 was examined with a reference of growth of *Synechococcus* PCC 7002. In the absence of ferric citrate as the Fe source as an essential nutrient, JNT 01 grew in the presence of Fe(II) ions but the growth of PCC 7002 was generally low and variable. This suggests that JNT 01 can use Fe(II) ions, or Fe(III) ions produced by oxidation more properly for growth as a nutrient,

whereas PCC 7002 cannot. This may relate to the adaptation of JNT 01 to the Fe(II)-rich environments of the hot springs. When ferric citrate was supplied in the growth medium after autoclaving, similar growth was observed between the growth of JNT 01 and PCC 7002 after 48 hours from the start of culture with Fe(II). The lack of difference at these later time points is probably related to the oxidation of all Fe(II) in the culture before 48 hours (compare Fig 7 g, h, Fig. 13 g, h).

The initial growth of JNT 01 and PCC 7002 was compared in 1000 μM Fe(II) at the beginning, under conditions where Fe(II) was still present until 48 hours after inoculation although the concentration was decreasing probably because of the oxygen evolved from the cyanobacteria. Significant growth was observed with JNT 01 but not observed with PCC 7002. Previous studies have demonstrated that Fe(II) ions in the growth medium affected the growth of cyanobacteria from low Fe(II) environments (e.g. Swanner et al., 2015). The finding of this study suggests that JNT01 from Fe(II)-rich environments was somewhat tolerant to Fe(II) but PCC 7002 was not.

There have been no reports about Fe(II) toxicity to cyanobacteria which were obtained from Fe(II)-rich environments. The results of this study suggest that as in the present-day iron rich hot springs as Jinata hot springs, ancient ocean with high-concentrations of Fe(II) may be a good habitat of cyanobacteria evolving oxygen molecules even though the presence of both of Fe(II) and molecular oxygen is toxic to living cells. How this is achieved remains unknown, but perhaps it is possible through tolerance mechanisms against the toxicity.

7. References

1. Achilles, K.M., Church, T.M., Wilhelm, S.W., Luther III, G., Hutchins, D.A., 2003. Bioavailability of iron to Trichodesmium colonies in the western subtropical Atlantic Ocean. Limnol. Oceanogr. 48, 2250–2255.
2. Anbar, A.D., Duan, Y., Lyons, T.W., Arnold, G.L., Kendall, B., Creaser, R.A., Kaufman, A.J., Gordon, G.W., Scott, C., Garvin, J., Buick, R., 2007. A Whiff of Oxygen Before the Great Oxidation Event? Science 317, 1903–1906. https://doi.org/10.1126/science.1140325
3. Barbeau, K., Rue, E.L., Bruland, K.W., Butler, A., 2001. Photochemical cycling of iron in the surface ocean mediated by microbial iron (III)-binding ligands. Nature 413, 409–413.
4. Bekker, A., Holland, H.D., Wang, P.-L., Iii, D.R., Stein, H.J., Hannah, J.L., Coetzee, L.L., Beukes, N.J., 2004. Dating the rise of atmospheric oxygen. Nature 427, 117. https://doi.org/10.1038/nature02260
5. Boone, D.R., Castenholz, R.W., 2012. Bergey's Manual of Systematic Bacteriology: Volume One : The Archaea and the Deeply Branching and Phototrophic Bacteria. Springer Science & Business Media.
6. Brown, I.I., Mummey, D., Cooksey, K.E., 2005. A novel cyanobacterium exhibiting an elevated tolerance for iron. FEMS Microbiol. Ecol. 52, 307–314. https://doi.org/10.1016/j.femsec.2004.11.020
7. Cairns-Smith, A.G., 1978. Precambrian solution photochemistry, inverse segregation, and banded iron formations. Nature 276, 807–808. https://doi.org/10.1038/276807a0
8. Camacho, A., Walter, X.A., Picazo, A., Zopfi, J., 2017. Photoferrotrophy: Remains of an Ancient Photosynthesis in Modern Environments. Front. Microbiol. 8. https://doi.org/10.3389/fmicb.2017.00323
9. Canfield, D.E., 1998. A new model for Proterozoic ocean chemistry. Nature 396, 450–453.
10. Choudhary, M., Jetley, U.K., Abash Khan, M., Zutshi, S., Fatma, T., 2007. Effect of heavy metal stress on proline, malondialdehyde, and superoxide dismutase activity in the cyanobacterium Spirulina platensis-S5. Ecotoxicol. Environ. Saf. 66, 204–209. https://doi.org/10.1016/j.ecoenv.2006.02.002
11. Claire, M.W., Catling, D.C., Zahnle, K.J., 2006. Biogeochemical modelling of the rise in atmospheric oxygen. Geobiology 4, 239–269.
12. Cloud, P.E., 1968. Atmospheric and hydrospheric evolution on the primitive Earth. Science 160, 729–736.
13. Debelius, B., Forja, J.M., DelValls, T.A., Lubián, L.M., 2009. Toxicity of copper in natural marine picoplankton populations. Ecotoxicol. Lond. Engl. 18, 1095–1103. https://doi.org/10.1007/s10646-009-0377-3

14. Farquhar, J., Zerkle, A.L., Bekker, A., 2011. Geological constraints on the origin of oxygenic photosynthesis. Photosynth. Res. 107, 11–36.
15. Hirata, D., Yamashita, H., Suzuki, K., Hirata, Y., Bing, Y., 2010. Collision accretion tectonics of the proto-Izu–Mariana Arc: a review. J Geogr. 119, 1125–1160.
16. Holland, H.D., 2003. The Geologic History of Seawater. Treatise Geochem. 6, 625. https://doi.org/10.1016/B0-08-043751-6/06122-3
17. Kappler, A., Pasquero, C., Konhauser, K.O., Newman, D.K., 2005. Deposition of banded iron formations by anoxygenic phototrophic Fe (II)-oxidizing bacteria. Geology 33, 865–868.
18. Konhauser, K.O., Hamade, T., Raiswell, R., Morris, R.C., Ferris, F.G., Southam, G., Canfield, D.E., 2002. Could bacteria have formed the Precambrian banded iron formations? Geology 30, 1079–1082.
19. Lane, D. J., 1991. 16S/23S rRNA sequencing, In E. Stackebrandt and M. Goodfellow (ed.), Nucleic acids techniques in bacterial systematics. John Wiley & Sons, Chichester, United Kingdom.
20. Lyons, T.W., Reinhard, C.T., Planavsky, N.J., 2014. The rise of oxygen in Earth's early ocean and atmosphere. Nature 506, 307–315. https://doi.org/10.1038/nature13068
21. Michel, K.-P., Pistorius, E.K., 2004. Adaptation of the photosynthetic electron transport chain in cyanobacteria to iron deficiency: the function of IdiA and IsiA. Physiol. Plant. 120, 36–50.
22. Miller, S.R., Castenholz, R.W., 2000. Evolution of Thermotolerance in Hot Spring Cyanobacteria of the Genus Synechococcus. Appl. Environ. Microbiol. 66, 4222–4229. https://doi.org/10.1128/AEM.66.10.4222-4229.2000
23. Muyzer, G., Ramsing, N.B., 1995. Molecular methods to study the organization of microbial communities. Water Sci. Technol., Biofilm Structure, Growth and Dynamics 32, 1–9. https://doi.org/10.1016/0273-1223(96)00001-7
24. Myers, J.L., Sekar, R., Richardson, L.L., 2007. Molecular Detection and Ecological Significance of the Cyanobacterial Genera Geitlerinema and Leptolyngbya in Black Band Disease of Corals. Appl. Environ. Microbiol. 73, 5173–5182. https://doi.org/10.1128/AEM.00900-07
25. Noll, M., Matthies, D., Frenzel, P., Derakshani, M., Liesack, W., 2005. Succession of bacterial community structure and diversity in a paddy soil oxygen gradient. Environ. Microbiol. 7, 382–395. https://doi.org/10.1111/j.1462-2920.2005.00700.x
26. Nübel, U., Garcia-Pichel, F., Muyzer, G., 1997. PCR primers to amplify 16S rRNA genes from cyanobacteria. Appl. Environ. Microbiol. 63, 3327–3332.
27. Pierson, B.K., Parenteau, M.N., Griffin, B.M., 1999. Phototrophs in High-Iron-Concentration Microbial Mats: Physiological Ecology of Phototrophs in an Iron-Depositing

Hot Spring. Appl. Environ. Microbiol. 65, 5474–5483.

28. Pierella Karlusich, J.J., Ceccoli, R., Graña, M., Romero, H., Carrillo, N., 2015. Environmental Selection Pressures Related to Iron Utilization Are Involved in the Loss of the Flavodoxin Gene from the Plant Genome. https://doi.org/10.1093/gbe/evv031
29. Planavsky, N.J., McGoldrick, P., Scott, C.T., Li, C., Reinhard, C.T., Kelly, A.E., Chu, X., Bekker, A., Love, G.D., Lyons, T.W., 2011. Widespread iron-rich conditions in the mid-Proterozoic ocean. Nature 477, 448–451.
30. Poulton, S.W., Canfield, D.E., 2011. Ferruginous Conditions: A Dominant Feature of the Ocean through Earth9s History. Elements 7, 107–112.
31. Rai, L.C., Gaur, J.P., Kumar, H.D., 1981. Phycology and Heavy-Metal Pollution. Biol. Rev. 56, 99–151. https://doi.org/10.1111/j.1469-185X.1981.tb00345.x
32. Rantamäki, S., Meriluoto, J., Spoof, L., Puputti, E.-M., Tyystjärvi, T., Tyystjärvi, E., 2016. Oxygen produced by cyanobacteria in simulated Archaean conditions partly oxidizes ferrous iron but mostly escapes-conclusions about early evolution. Photosynth. Res. 130, 103–111. https://doi.org/10.1007/s11120-016-0231-4
33. Stookey, L.L., 1970. Ferrozine-A New Spectrophotometric Reagent for Iron. Anal. Chem. 42, 779–781. https://doi.org/10.1021/ac60289a016
34. Straus NA, 1994. Heterocyst metabolism and development, In Bryant DA, editor. (ed), The molecular biology of cyanobacteria. Kluwer Academic Publishers, Dordrecht, Netherlands.
35. Suzuki, M.T., Giovannoni, S.J., 1996. Bias caused by template annealing in the amplification of mixtures of 16S rRNA genes by PCR. Appl. Environ. Microbiol. 62, 625–630.
36. Swanner, E., Wu, W., Hao, L., Wuestner, M., Obst, M., Moran, D., McIlvin, M., Saito, M., Kappler, A., 2015. Physiology, Fe(II) oxidation, and Fe mineral formation by a marine planktonic cyanobacterium grown under ferruginous conditions. Front. Earth Sci. 3, 60. https://doi.org/10.3389/feart.2015.00060
37. Swanner, E.D., Mloszewska, A.M., Cirpka, O.A., Schoenberg, R., Konhauser, K.O., Kappler, A., 2015. Modulation of oxygen production in Archaean oceans by episodes of Fe (II) toxicity. Nat. Geosci. 8, 126–130.
38. Tangalos, G.E., Beard, B.L., Johnson, C.M., Alpers, C.N., Shelobolina, E.S., Xu, H., Konishi, H., Roden, E.E., 2010. Microbial production of isotopically light iron (II) in a modern chemically precipitated sediment and implications for isotopic variations in ancient rocks. Geobiology 8, 197–208.
39. Trouwborst, R.E., Johnston, A., Koch, G., Luther, G.W., Pierson, B.K., 2007. Biogeochemistry of Fe (II) oxidation in a photosynthetic microbial mat: implications for Precambrian Fe (II) oxidation. Geochim. Cosmochim. Acta 71, 4629–4643.

8. Tables and Figures

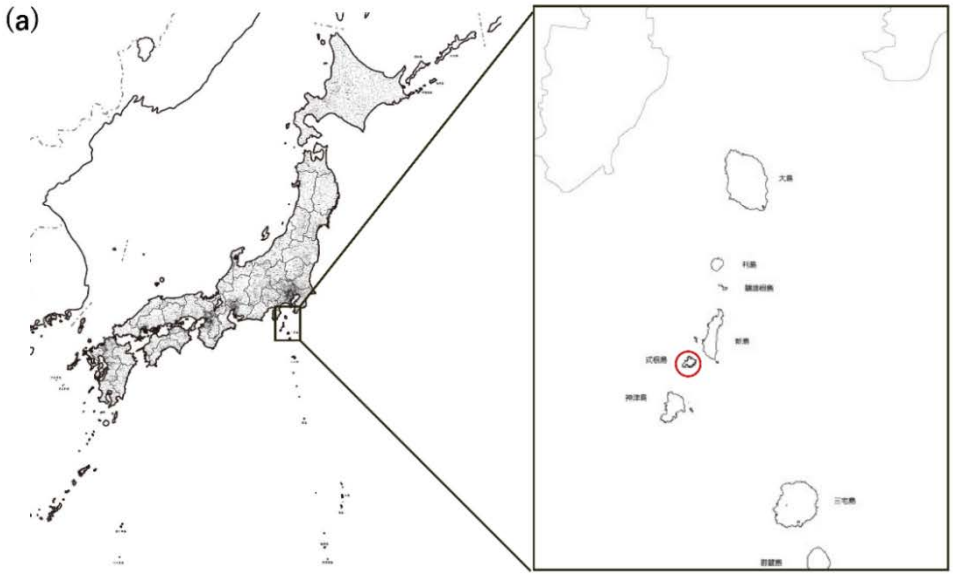

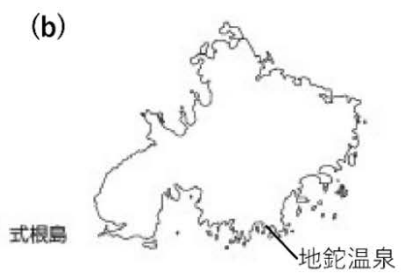

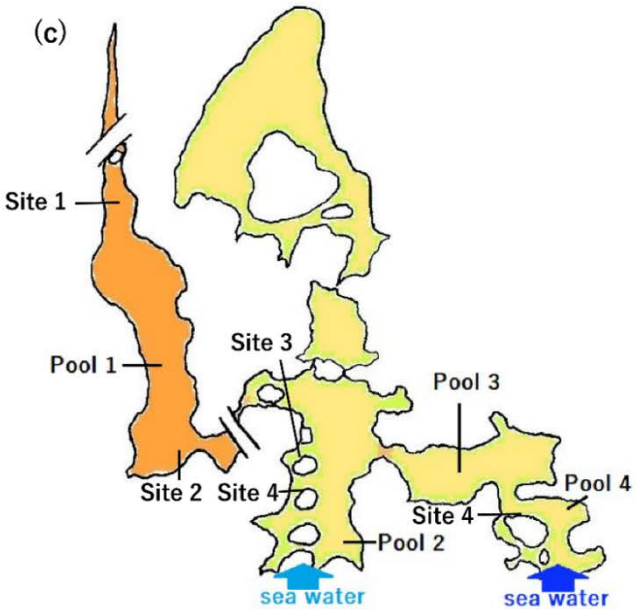


(f)


(g)


(h)


(i)


(j)


(k)


(l)

Fig. 1 Map of Jinata hot spring and sampling site. (a) Site of Shikine-island in map of Japan. (b) Jinata hot spring is located on the coast of Shikine-island. (c) Map of Jinata hot spring was traced. (d) and (e) Pool 1 water was merging at high tide. There are three pools, Pool 2, 3 (f) and Pool 4 (h) below the source pool. (h) Site 1 was the deep part (50 cm) of the sourse. (i) Site 2 contained streamers with orange minerals, which were unique structures of bacteria. (j) In Site 3 there are three main layers. The top was green mat and the second was an orange layer. The bottom was black layer. (k) Site 4 was similar to site 3. (l) Site 5 contained green mats and bubbles. Under the mat, there was fluffy orange sediment.

Table 1 The temperature, pH and concentration of ferrous iron at each site at high tide.

Site	pH	T (°C)	DO (μM)	Fe(II) (μM)
1	5.4	63-66	4.7(source) 39(surface)	261
2	5.8	60.5	58	171
3	6.5	54.6	134	180
4	6.7	54.9	NA	183
5	6.5	51.7	234	91

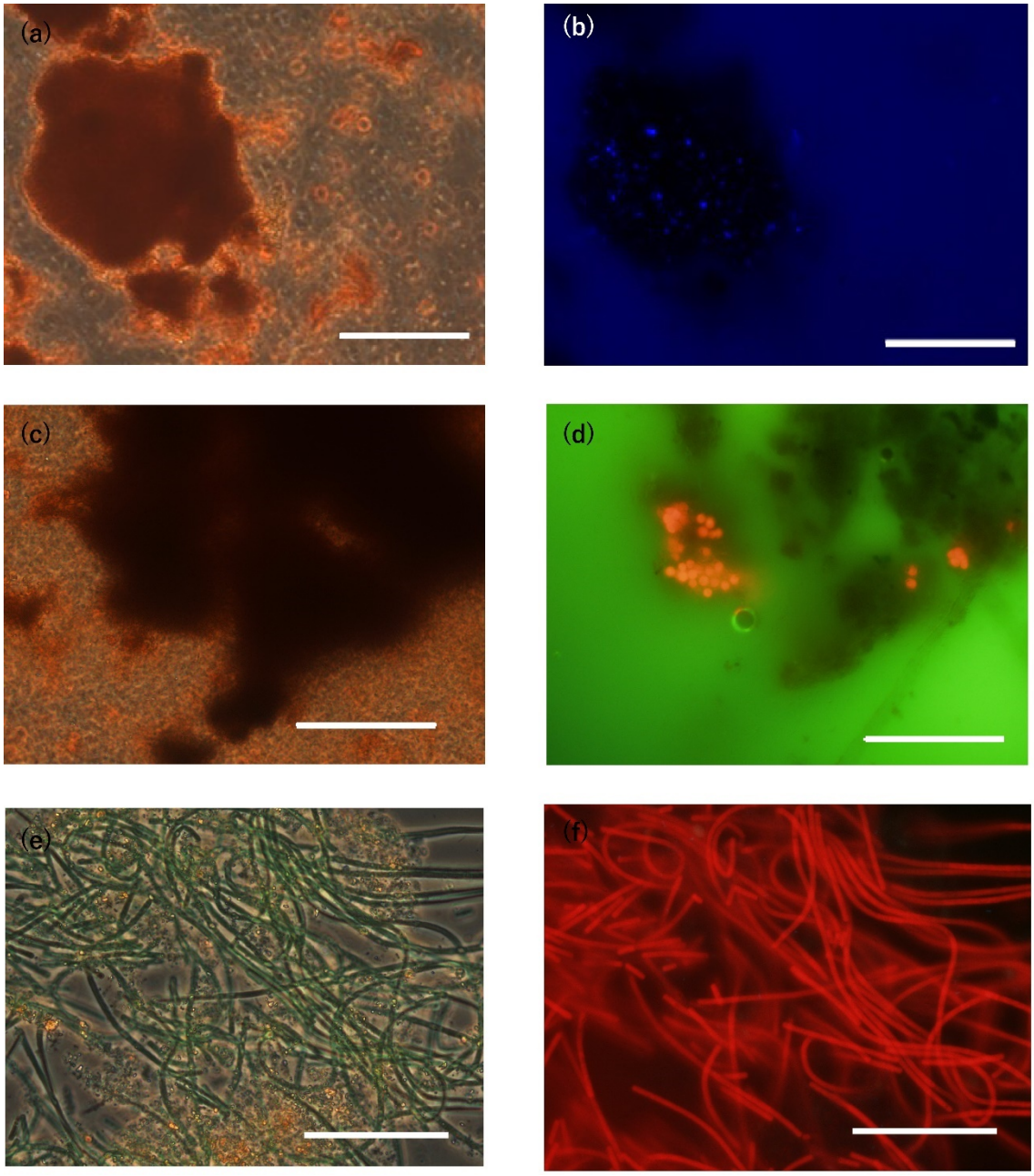

Fig. 2 Microscopy images of orange sediment and green mat at site 1, 3, 5. The pictures on the left (a, c, e) are light microscopy images. The image of orange particles of Site 1 is (a). (b) indicated the same field of (a) is the DAPI fluorescence image. The blue signal is DAPI-stained cells (Excitation: 365 nm, Emission: BP 445~50 nm). (c) is the image of Site 3 sample which were orange and black deposits without green mats. (f) is the image of the microbial mat of Site 5. The red color of fluorescence images (d, f) observed on the same fields of (c, e) is autofluoresence signal of cyanobacteria (BP 395~440 nm, LP 470 nm). Bar, 50 μm.

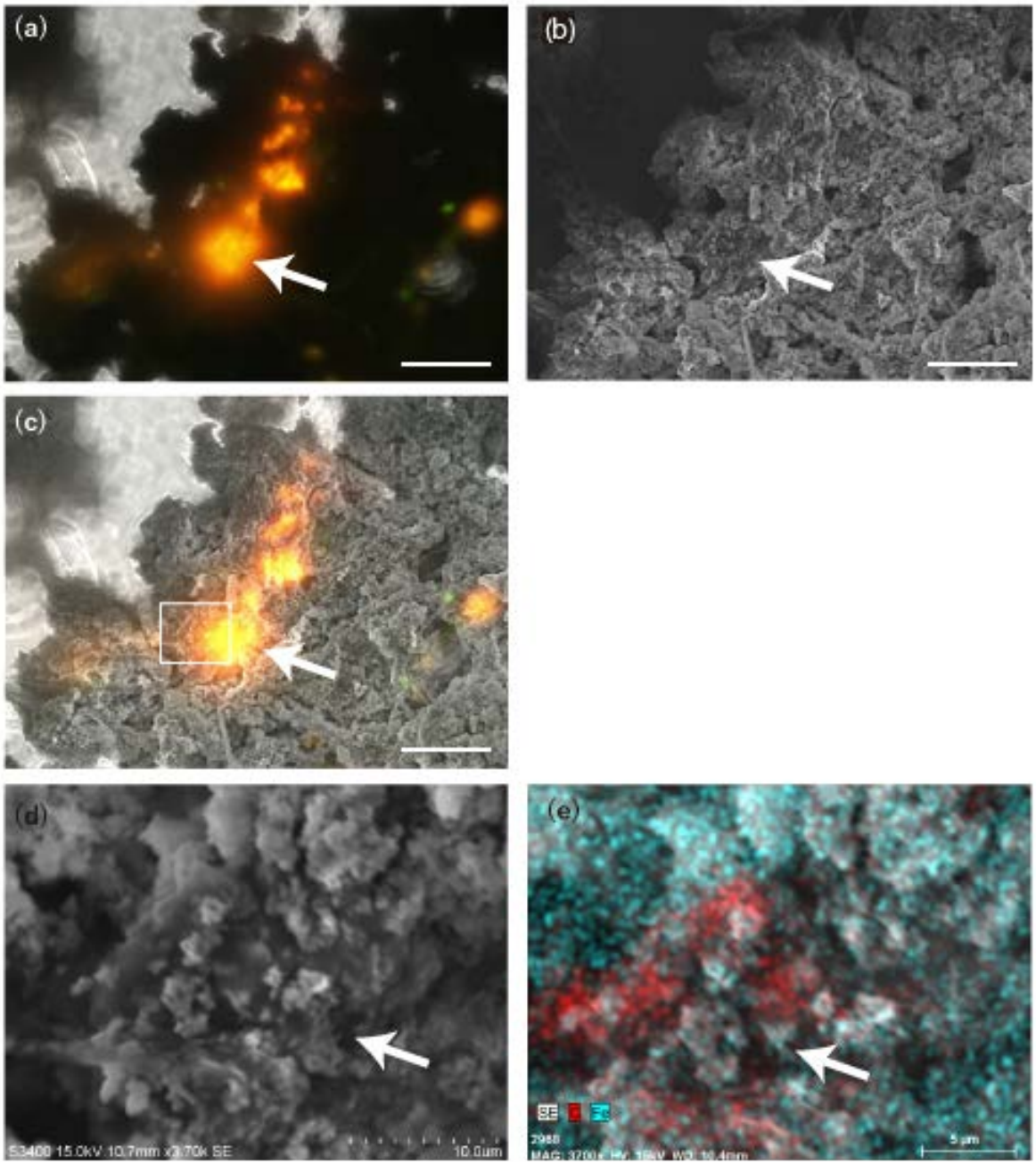

Fig. 3 Identification of cyanobacteria in SEM image and EDS image. White arrows indicate cyanobacteria. (a) Merge images of Light and fluorescence microscopy. The black layer of site3 (b) SEM image of same field as (a). Bar, 50μm. (c) merge image (a) and (b). (d) SEM images focus on cyanobacteria signal of a part of the white square in (c). Bar, 10μm. (e) EDS analysis: Red spots indicate areas of high carbon content.. Sky blue spots shows the inclusion of iron.

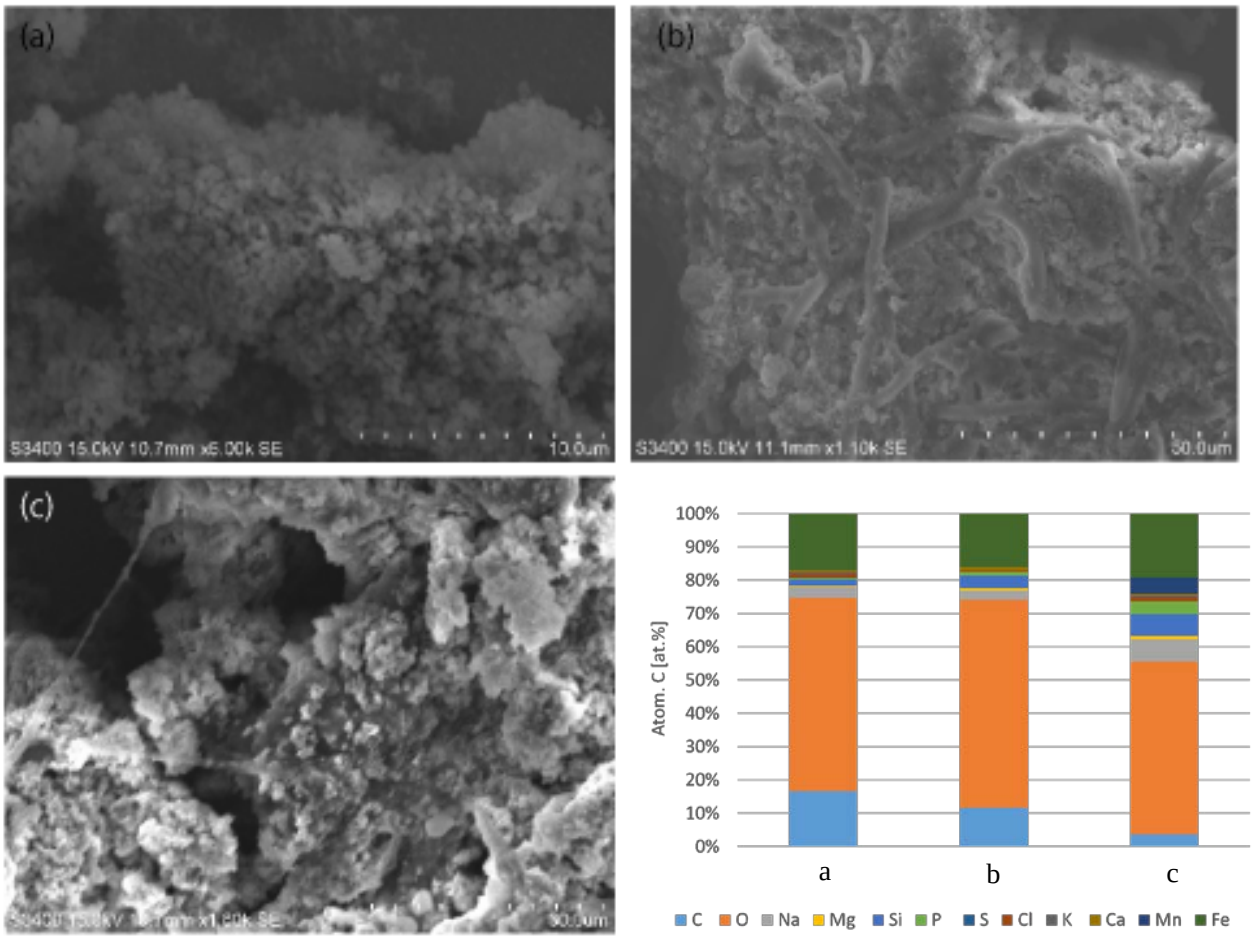

Fig. 4 Mineral compound measured by SEM-EDS. (a), (b) and (c) are SEM images. (a) The orange particles from site1. (b) The filamentous structures are cyanobacteria in green mat from site5. (c) The black layer contained unicellular cyanobacteria from site3. (d) Average of mineral compound from random 10 spots in (a)-(c).

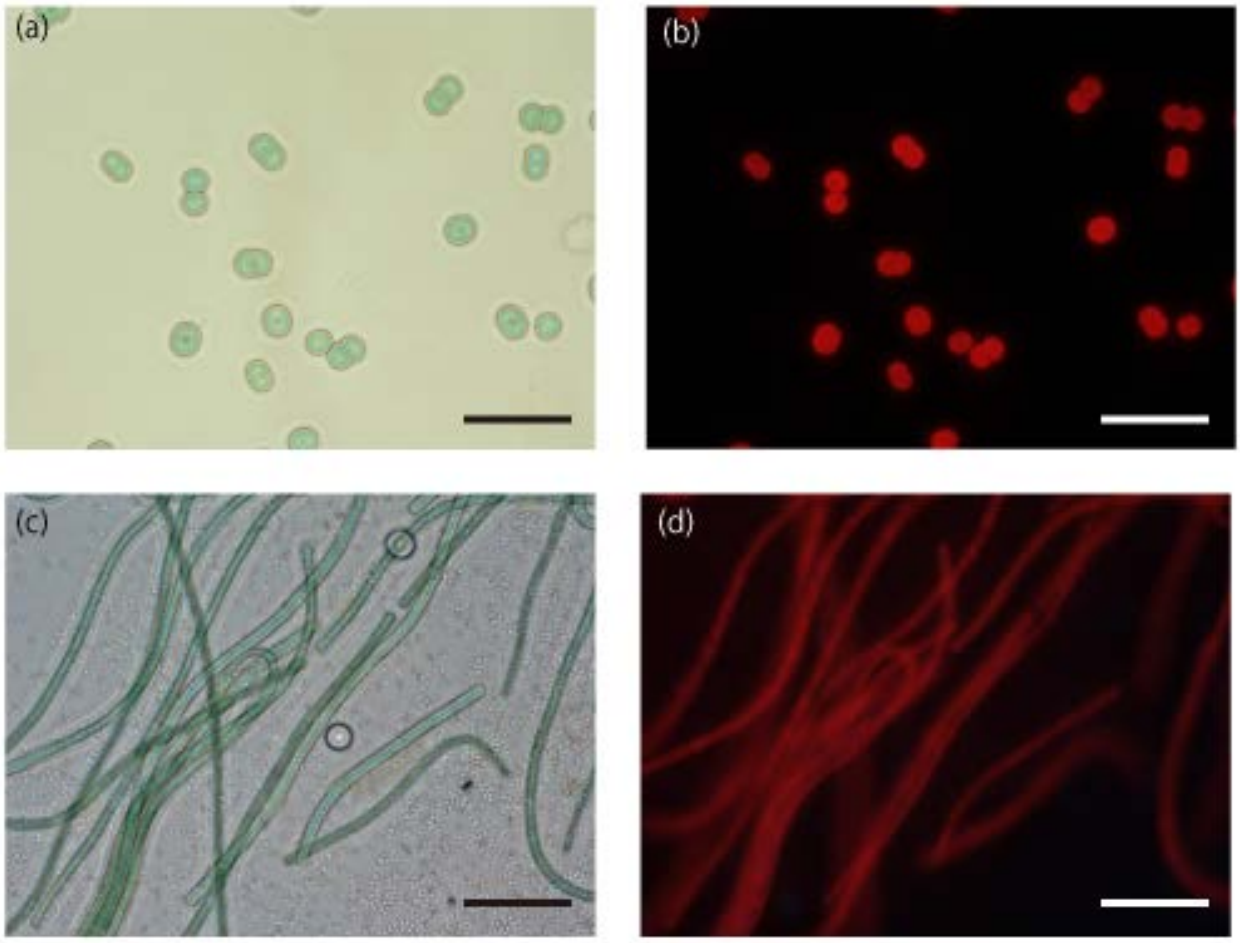

Fig. 5 Two types of enrichment cultures contained cyanobacteria. (a) Light microscopy image of the unicellular cyanobacteria JNT 01 (b) Fluorescence microscopy image of the same field of (a). (c) filamentous cyanobacteria JNT 02. (d) Fluorescence image of the same field of (c). Bar is 20 µm

Table 2 Primer sets

Targeted gene	Primer set	Sequence	Reference
16S rRNA	27F	5’ -AGAGTTTGATCMTGGCTCAG- 3’	(Suzuki and Giovannoni, 1996)
	907R	5'-CCGTCAATTCCTTTRAGTTT-3'	(Muyzer and Ramsing, 1995)
	1427R	5'-TACGGYTACCTTGTTACGACTT-3'	(Lane, D. J., 1991)
16S rRNA specific for cyanobacteria	CYA106F	5'-CGGACGGGTGAGTAACGCGTGA -3'	(Nübel et al., 1997)
	PLG 2.3	5'-CTTCAYGYAGGCGAGTTGCAGC -3'	(Miller and Castenholz, 2000)

Table 3 16S rRNA gene sequences

	Related strain	Similarity	Accession number	References
JNT 01	*Cyanobacterium aponinum* strain PCC 10605	99%	CP003947	Pierella Karlusich et al., (2015)
JNT 02	*Geitlerinema* sp. BBD_P2b-1	99%	EF372580	Myers,J.L. et al (2007)

Fig. 6 Images of cultivation system in anoxic, air-tight bottles with different concentration of Fe (II) at the beginning. These images were the 5 days cultures of *Synechococcus* PCC 7002.

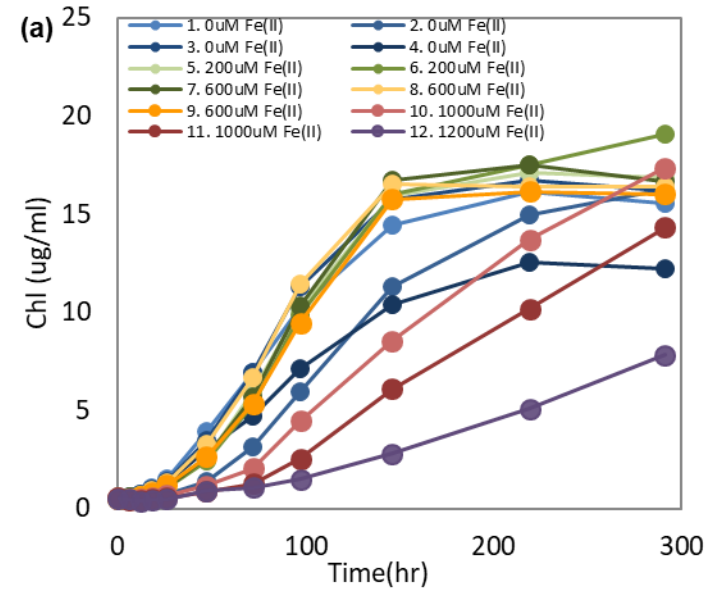
(a)
Chl (ug/ml)
Time(hr)
1. 0uM Fe(II)
2. 0uM Fe(II)
3. 0uM Fe(II)
4. 0uM Fe(II)
5. 200uM Fe(II)
6. 200uM Fe(II)
7. 600uM Fe(II)
8. 600uM Fe(II)
9. 600uM Fe(II)
10. 1000uM Fe(II)
11. 1000uM Fe(II)
12. 1200uM Fe(II)

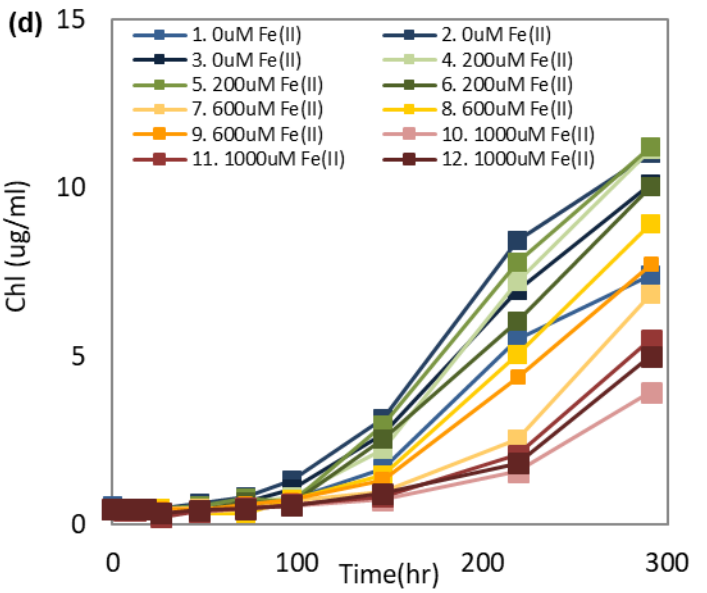
(d)
Chl (ug/ml)
Time(hr)
1. 0uM Fe(II)
2. 0uM Fe(II)
3. 0uM Fe(II)
4. 200uM Fe(II)
5. 200uM Fe(II)
6. 200uM Fe(II)
7. 600uM Fe(II)
8. 600uM Fe(II)
9. 600uM Fe(II)
10. 1000uM Fe(II)
11. 1000uM Fe(II)
12. 1000uM Fe(II)

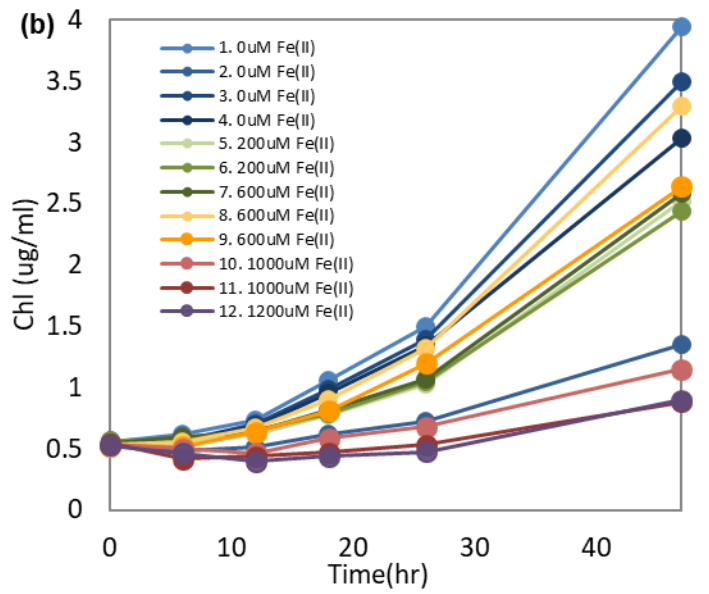
(b)
Chl (ug/ml)
Time(hr)
1. 0uM Fe(II)
2. 0uM Fe(II)
3. 0uM Fe(II)
4. 0uM Fe(II)
5. 200uM Fe(II)
6. 200uM Fe(II)
7. 600uM Fe(II)
8. 600uM Fe(II)
9. 600uM Fe(II)
10. 1000uM Fe(II)
11. 1000uM Fe(II)
12. 1200uM Fe(II)

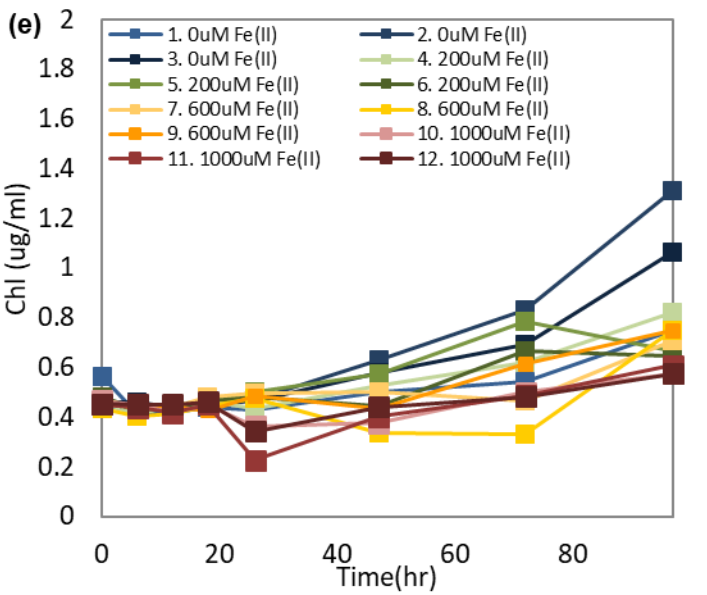
(e)
Chl (ug/ml)
Time(hr)
1. 0uM Fe(II)
2. 0uM Fe(II)
3. 0uM Fe(II)
4. 200uM Fe(II)
5. 200uM Fe(II)
6. 200uM Fe(II)
7. 600uM Fe(II)
8. 600uM Fe(II)
9. 600uM Fe(II)
10. 1000uM Fe(II)
11. 1000uM Fe(II)
12. 1000uM Fe(II)

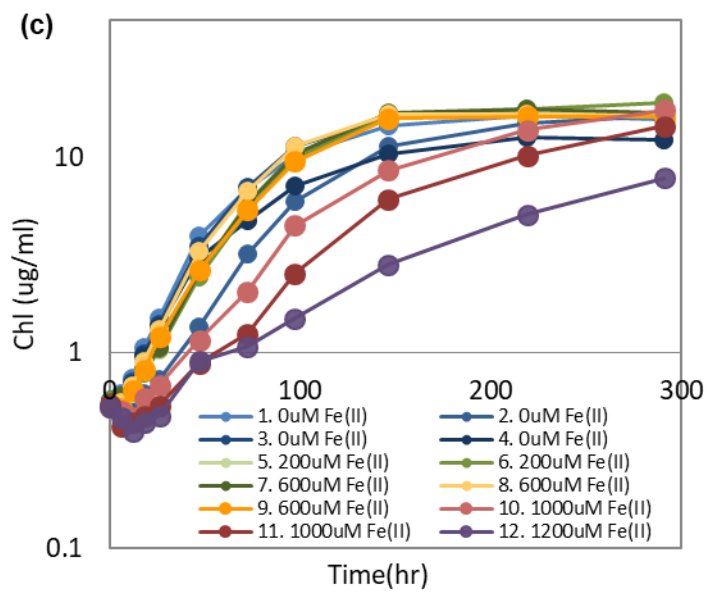
(c)
Chl (ug/ml)
Time(hr)
1. 0uM Fe(II)
2. 0uM Fe(II)
3. 0uM Fe(II)
4. 0uM Fe(II)
5. 200uM Fe(II)
6. 200uM Fe(II)
7. 600uM Fe(II)
8. 600uM Fe(II)
9. 600uM Fe(II)
10. 1000uM Fe(II)
11. 1000uM Fe(II)
12. 1200uM Fe(II)

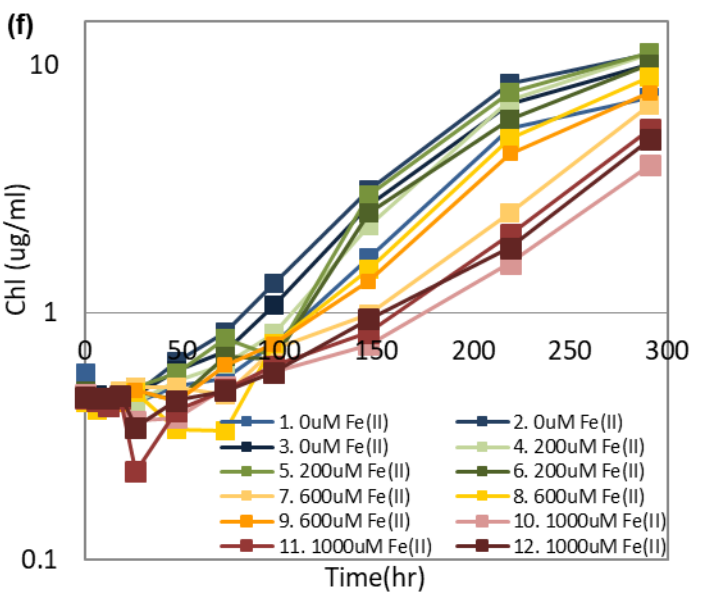
(f)
Chl (ug/ml)
Time(hr)
1. 0uM Fe(II)
2. 0uM Fe(II)
3. 0uM Fe(II)
4. 200uM Fe(II)
5. 200uM Fe(II)
6. 200uM Fe(II)
7. 600uM Fe(II)
8. 600uM Fe(II)
9. 600uM Fe(II)
10. 1000uM Fe(II)
11. 1000uM Fe(II)
12. 1000uM Fe(II)

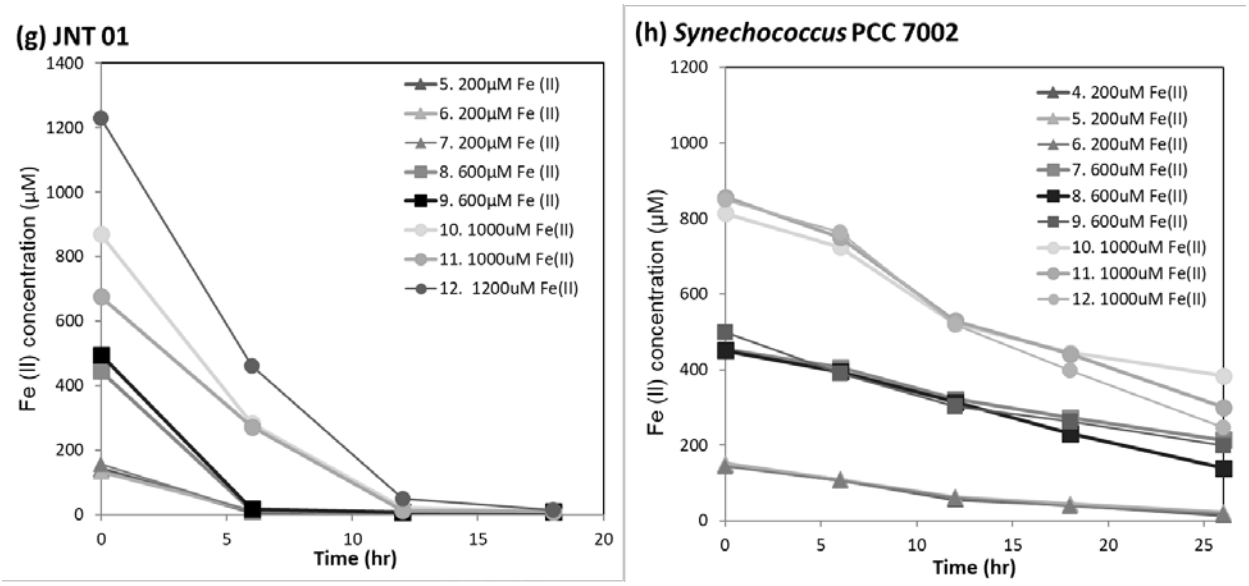

Fig. 7 Growth of JNT01 and *Synechococcus* PCC 7002 and Fe(II) concentration at different Fe(II) concentration. Initial cyanobacterial concentration inoculated was 0.5 μg/ml chlorophyll. Ferric ammonium citrate was added before autoclaving. (a) JNT01 growth curve, (b) close up (a), (c) the data from (a) were plotted on a log scaled axis. (d) *Synechococcus* PCC 7002 growth curve, (e) close up (d), (f) the data from (d) were plotted on a log scaled axis. (g) Fe(II) measurements from representative replicates of experiments where JNT 01 was grown under conditions that began anoxic with 200 μM (triangles), 600 μM (squares), 1000 μM and 1200 μM (circles) Fe(II). (h) Fe(II) measurements from *Synechococcus* PCC 7002.

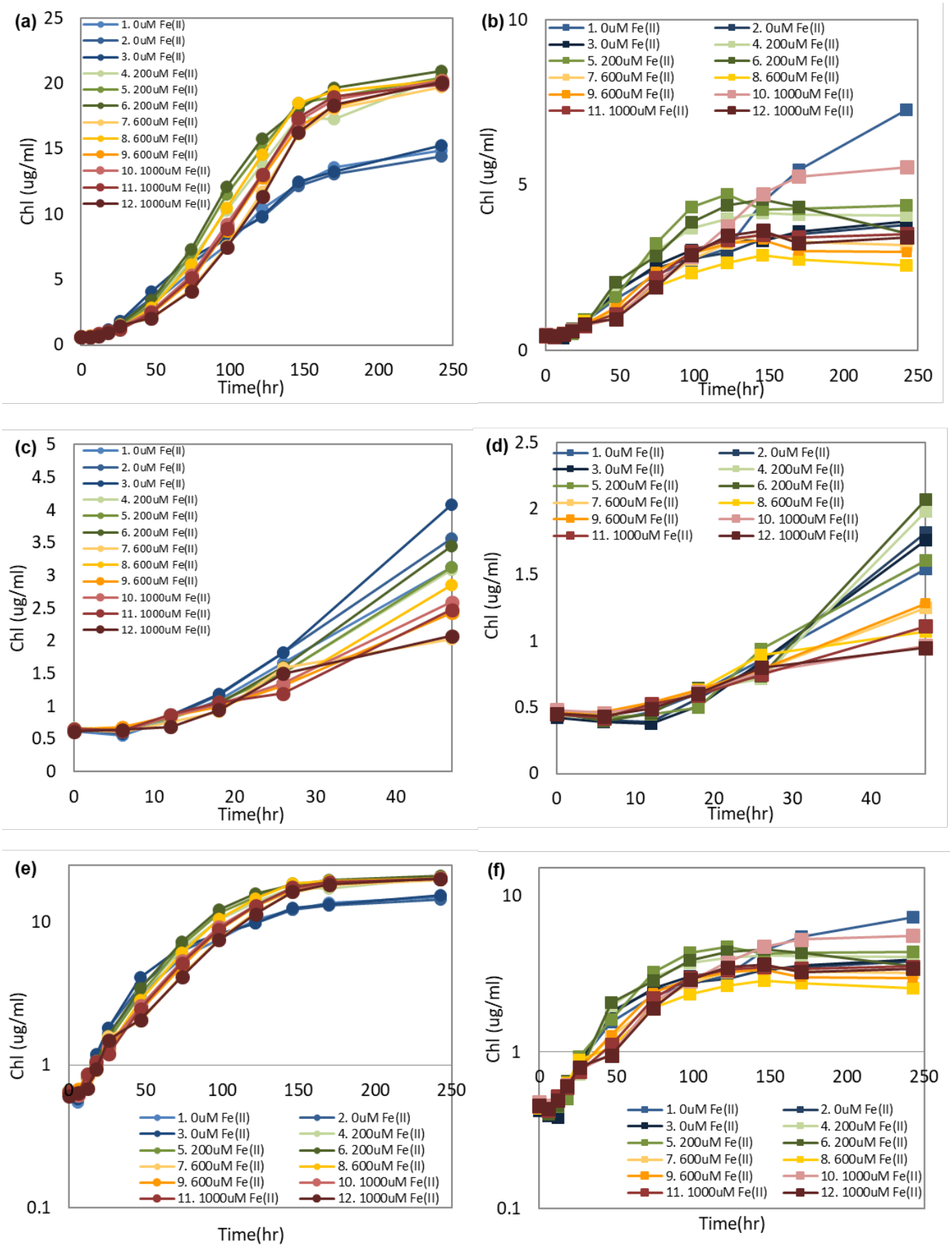
(a)
Chl (ug/ml)
Time(hr)
1. 0uM Fe(II)
2. 0uM Fe(II)
3. 0uM Fe(II)
4. 200uM Fe(II)
5. 200uM Fe(II)
6. 200uM Fe(II)
7. 600uM Fe(II)
8. 600uM Fe(II)
9. 600uM Fe(II)
10. 1000uM Fe(II)
11. 1000uM Fe(II)
12. 1000uM Fe(II)
(b)
Chl (ug/ml)
Time(hr)
(c)
Chl (ug/ml)
Time(hr)
(d)
Chl (ug/ml)
Time(hr)
(e)
Chl (ug/ml)
Time(hr)
(f)
Chl (ug/ml)
Time(hr)

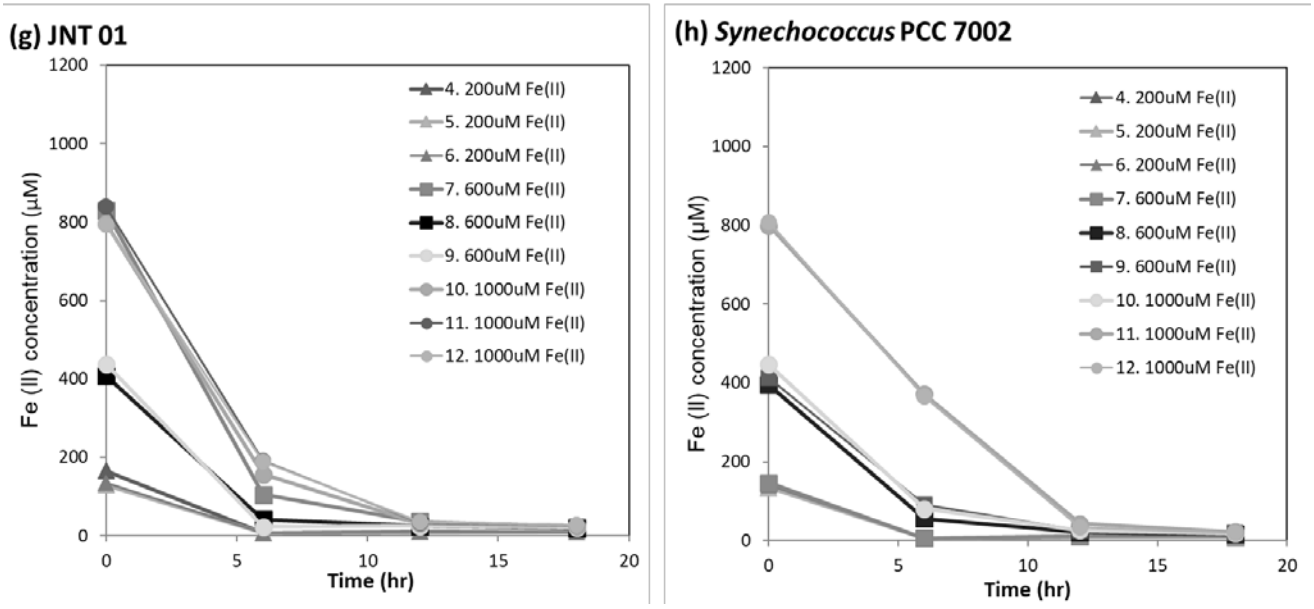

Fig. 8 Growth of JNT01 and *Synechococcus* PCC 7002 and Fe(II) concentration at different Fe(II) concentration. Experimental conditions were the same as in Fig. 7 Growth of JNT01 and Synechococcus PCC 7002 and Fe(II) concentration at different Fe(II) concentration. Initial cyanobacterial concentration inoculated was 0.5 μg/ml chlorophyll. Ferric ammonium citrate was added before autoclaving. (a) JNT01 growth curve, (b) close up (a), (c) the data from (a) were plotted on a log scaled axis. (d) Synechococcus PCC 7002 growth curve, (e) close up (d), (f) the data from (d) were plotted on a log scaled axis. (g) Fe(II) measurements from representative replicates of experiments where JNT 01 was grown under conditions that began anoxic with 200 μM (triangles), 600 μM (squares), 1000 μM and 1200 μM (circles) Fe(II). (h) Fe(II) measurements from *Synechococcus* PCC 7002.

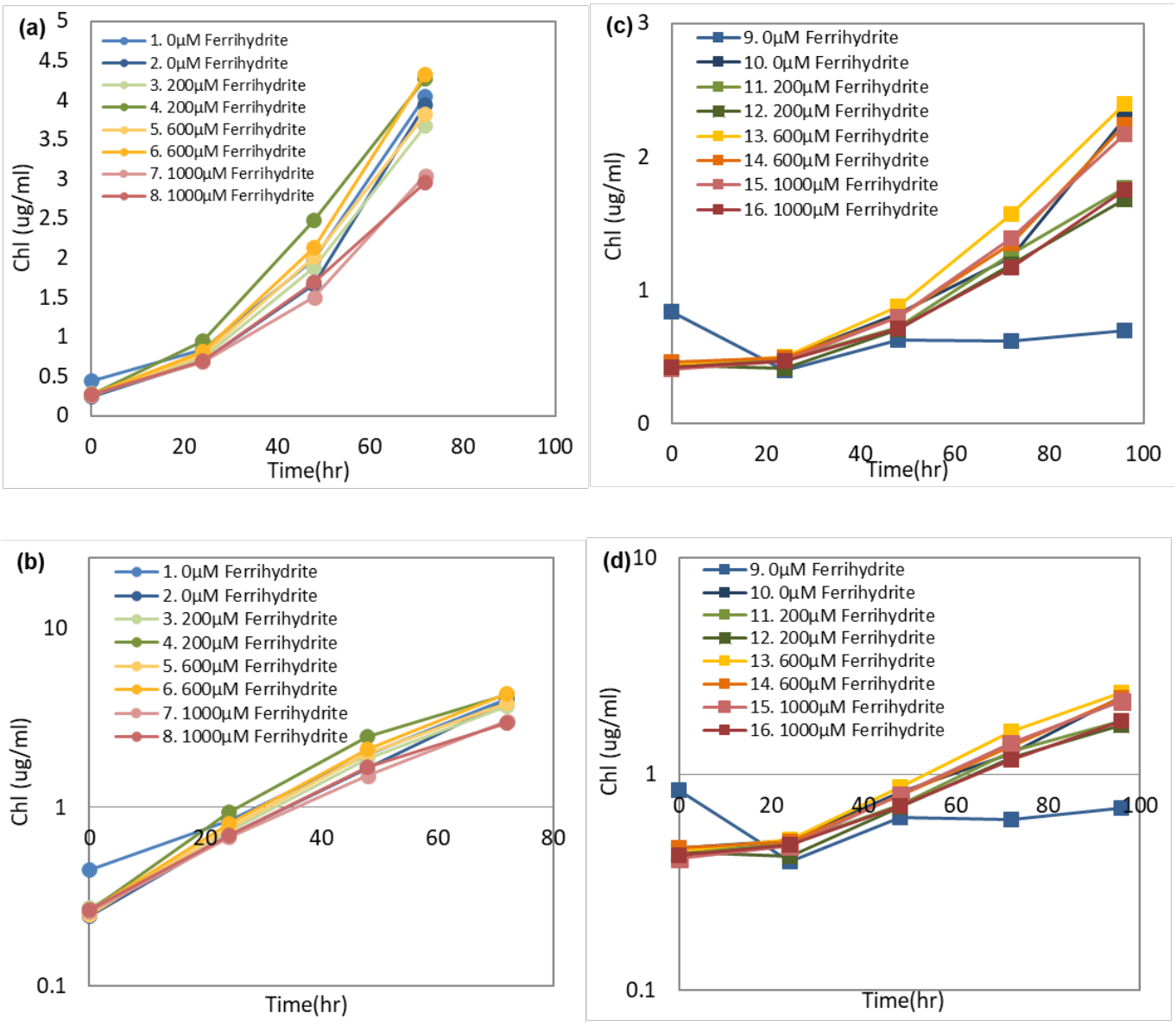

Fig. 9 Growth of JNT01 and *Synechococcus* PCC 7002 at different Ferrihydrite concentration. Initial cyanobacterial concentration inoculated was 0.5 μg/ml chlorophyll. Ferric ammonium citrate was added after autoclaving. (a) JNT01 growth curve, (b) the data from (a) were plotted on a log scaled axis. (c) *Synechococcus s* PCC 7002 growth curve, (d) the data from (c) were plotted on a log scaled axis.

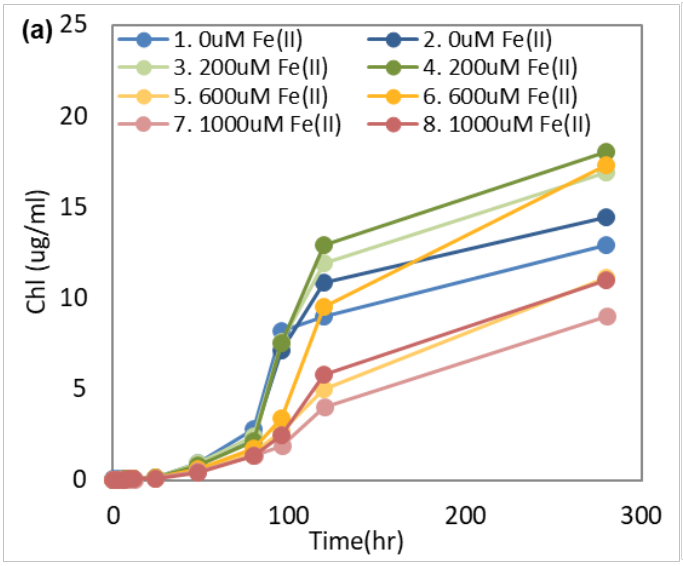
(a)
1. 0uM Fe(II)
2. 0uM Fe(II)
3. 200uM Fe(II)
4. 200uM Fe(II)
5. 600uM Fe(II)
6. 600uM Fe(II)
7. 1000uM Fe(II)
8. 1000uM Fe(II)
Chl (ug/ml)
Time(hr)

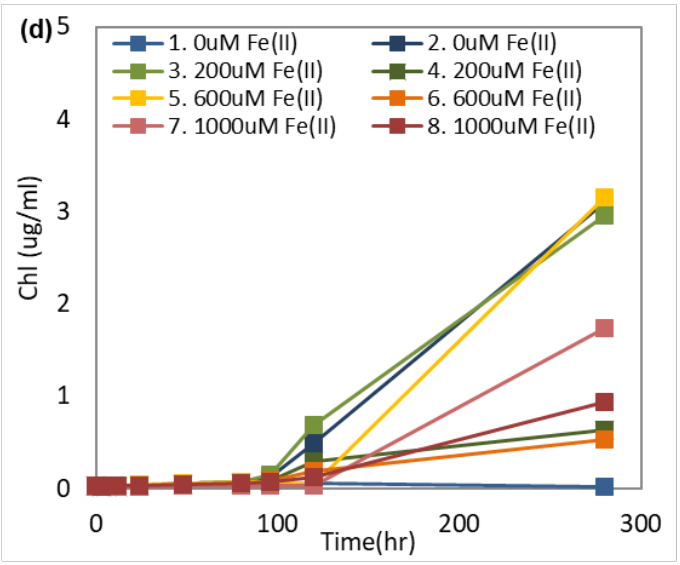
(d)
1. 0uM Fe(II)
2. 0uM Fe(II)
3. 200uM Fe(II)
4. 200uM Fe(II)
5. 600uM Fe(II)
6. 600uM Fe(II)
7. 1000uM Fe(II)
8. 1000uM Fe(II)
Chl (ug/ml)
Time(hr)

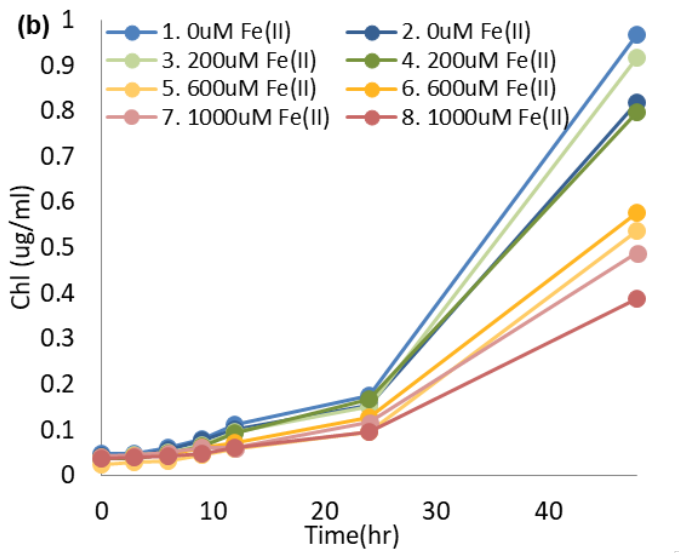
(b)
1. 0uM Fe(II)
2. 0uM Fe(II)
3. 200uM Fe(II)
4. 200uM Fe(II)
5. 600uM Fe(II)
6. 600uM Fe(II)
7. 1000uM Fe(II)
8. 1000uM Fe(II)
Chl (ug/ml)
Time(hr)

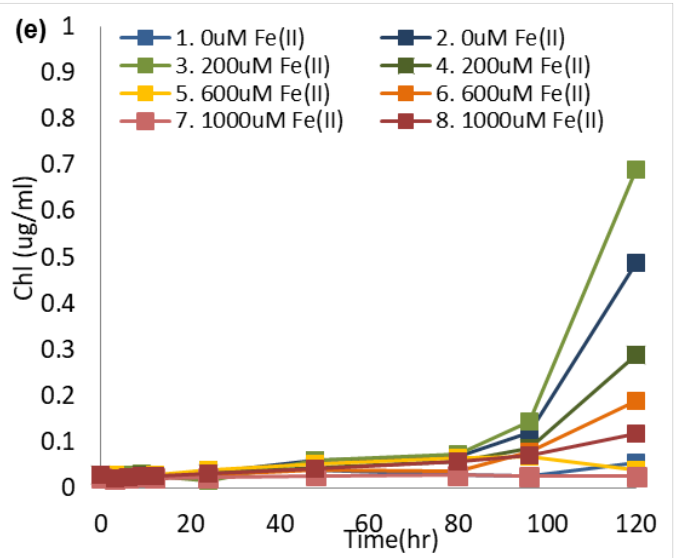
(e)
1. 0uM Fe(II)
2. 0uM Fe(II)
3. 200uM Fe(II)
4. 200uM Fe(II)
5. 600uM Fe(II)
6. 600uM Fe(II)
7. 1000uM Fe(II)
8. 1000uM Fe(II)
Chl (ug/ml)
Time(hr)

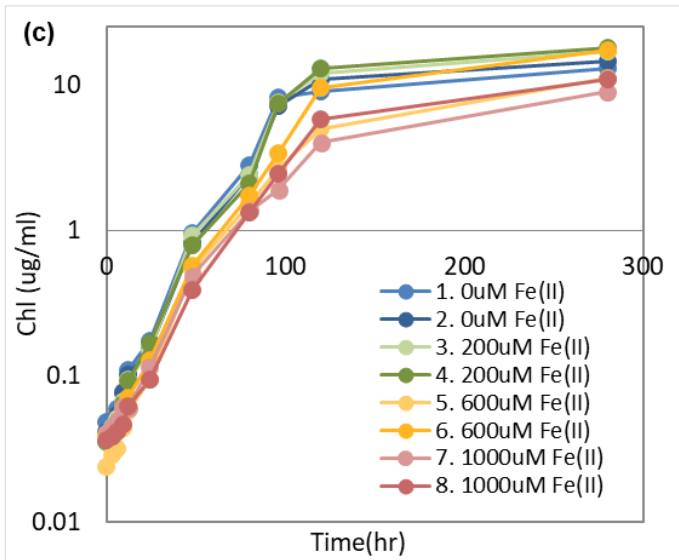
(c)
1. 0uM Fe(II)
2. 0uM Fe(II)
3. 200uM Fe(II)
4. 200uM Fe(II)
5. 600uM Fe(II)
6. 600uM Fe(II)
7. 1000uM Fe(II)
8. 1000uM Fe(II)
Chl (ug/ml)
Time(hr)

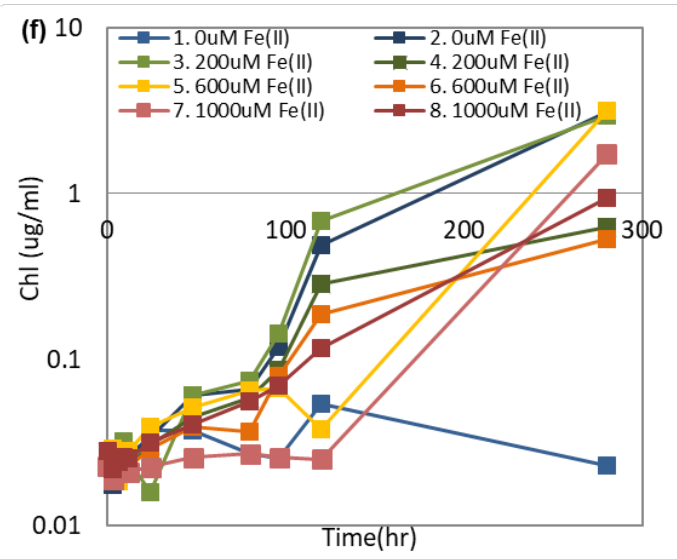
(f)
1. 0uM Fe(II)
2. 0uM Fe(II)
3. 200uM Fe(II)
4. 200uM Fe(II)
5. 600uM Fe(II)
6. 600uM Fe(II)
7. 1000uM Fe(II)
8. 1000uM Fe(II)
Chl (ug/ml)
Time(hr)

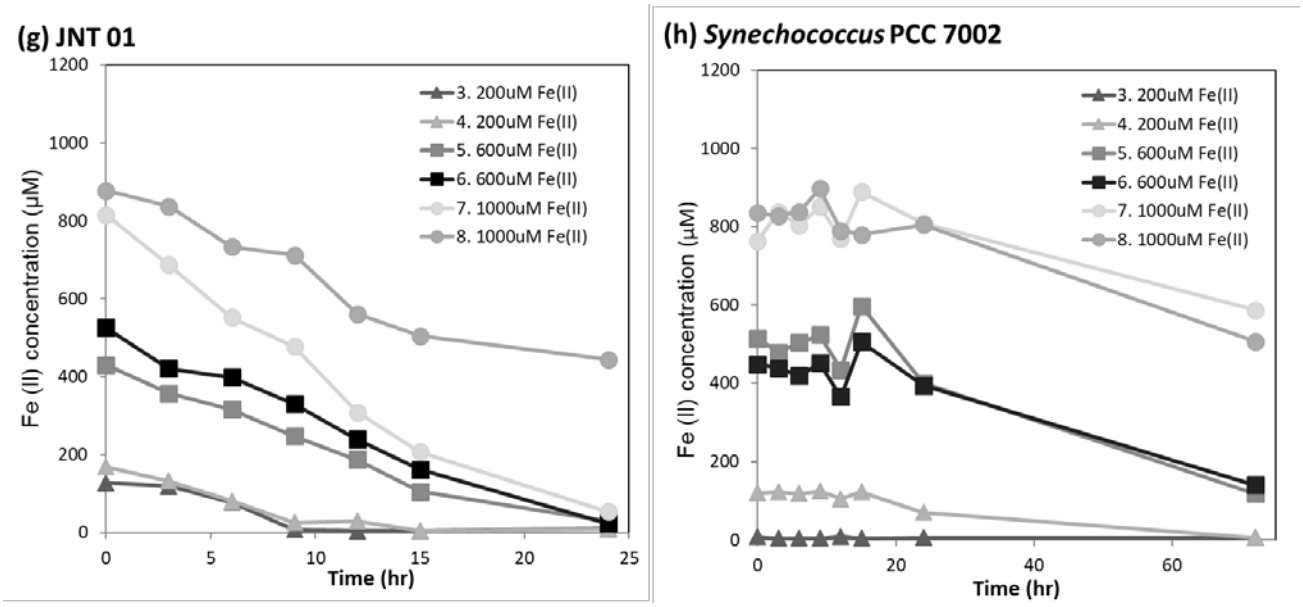

Fig. 10 Growth under the inoculation condition changed of JNT01 and *Synechococcus* PCC 7002 and Fe(II) concentration at different Fe(II) concentration. In the experiments, the cyanobacterial concentration inoculated was 0.05 μg/ml chlorophyll. Ferric ammonium citrate was added before autoclaving. (a) JNT01 growth curve, (b) close up (a), (c) the data from (a) were plotted on a log scaled axis. (d) *Synechococcus* PCC 7002 growth curve, (e) close up (d), (f) the data from (d) were plotted on a log scaled axis. (g) Fe(II) measurements from representative replicates of experiments where JNT 01 was grown under conditions that began anoxic with 200 μM (triangles), 600 μM (squares) 1000 μM(circles), initial Fe(II). (h) Fe(II) measurements of *Synechococcus* PCC 7002.

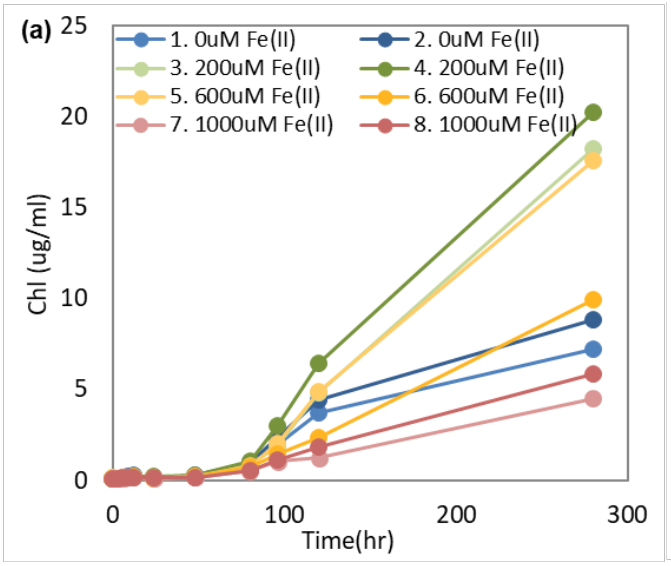
(a)
1. 0uM Fe(II)
2. 0uM Fe(II)
3. 200uM Fe(II)
4. 200uM Fe(II)
5. 600uM Fe(II)
6. 600uM Fe(II)
7. 1000uM Fe(II)
8. 1000uM Fe(II)
Chl (ug/ml)
Time(hr)

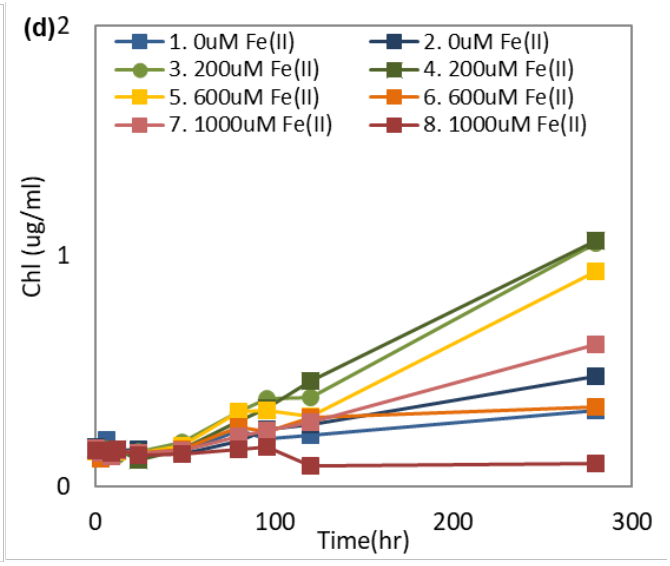
(d)
1. 0uM Fe(II)
2. 0uM Fe(II)
3. 200uM Fe(II)
4. 200uM Fe(II)
5. 600uM Fe(II)
6. 600uM Fe(II)
7. 1000uM Fe(II)
8. 1000uM Fe(II)
Chl (ug/ml)
Time(hr)

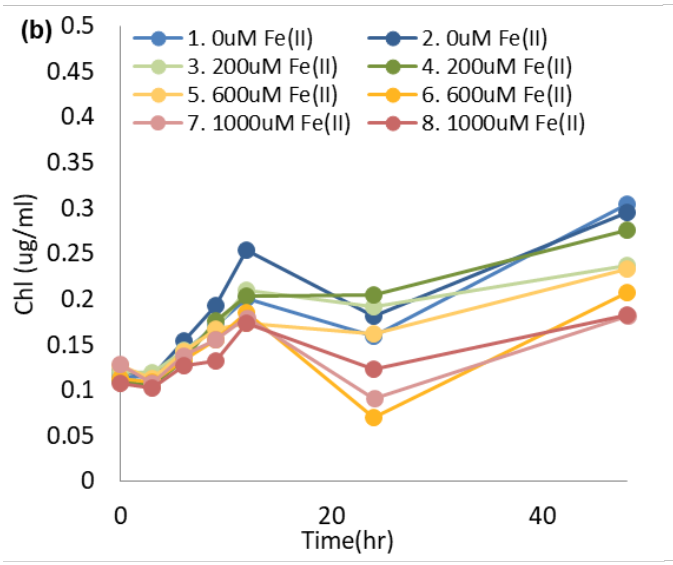
(b)
1. 0uM Fe(II)
2. 0uM Fe(II)
3. 200uM Fe(II)
4. 200uM Fe(II)
5. 600uM Fe(II)
6. 600uM Fe(II)
7. 1000uM Fe(II)
8. 1000uM Fe(II)
Chl (ug/ml)
Time(hr)

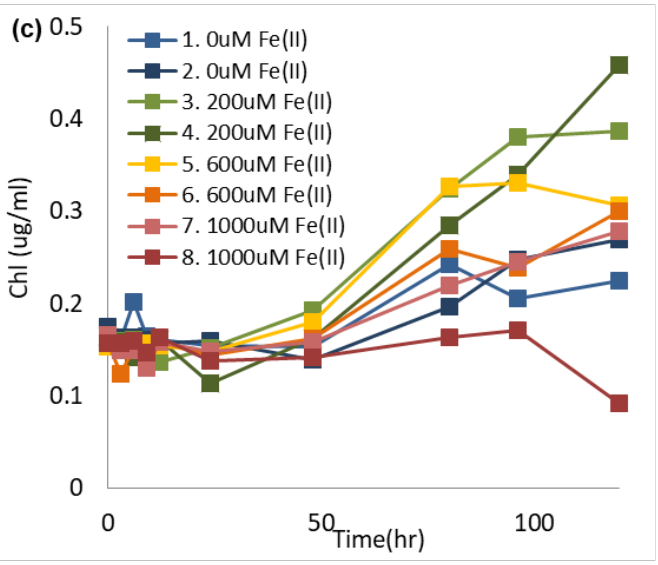
(c)
1. 0uM Fe(II)
2. 0uM Fe(II)
3. 200uM Fe(II)
4. 200uM Fe(II)
5. 600uM Fe(II)
6. 600uM Fe(II)
7. 1000uM Fe(II)
8. 1000uM Fe(II)
Chl (ug/ml)
Time(hr)

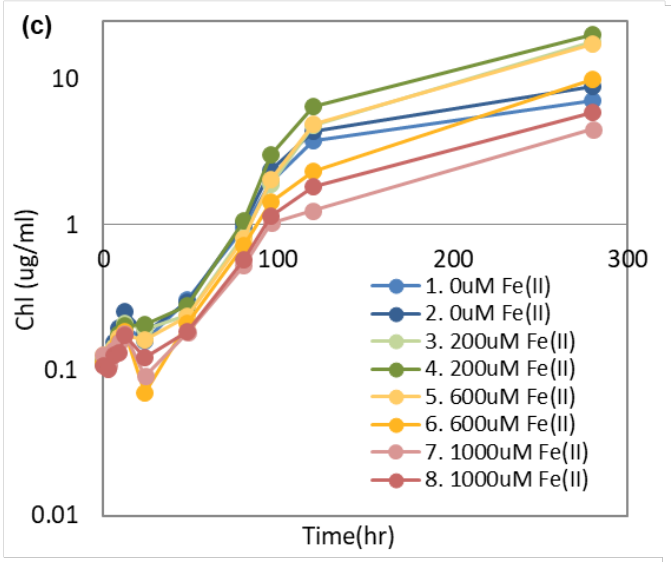
(c)
1. 0uM Fe(II)
2. 0uM Fe(II)
3. 200uM Fe(II)
4. 200uM Fe(II)
5. 600uM Fe(II)
6. 600uM Fe(II)
7. 1000uM Fe(II)
8. 1000uM Fe(II)
Chl (ug/ml)
Time(hr)

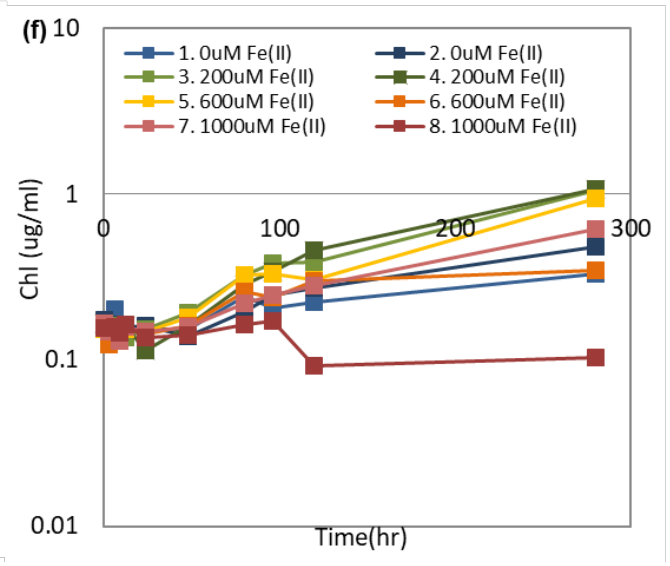
(f)
1. 0uM Fe(II)
2. 0uM Fe(II)
3. 200uM Fe(II)
4. 200uM Fe(II)
5. 600uM Fe(II)
6. 600uM Fe(II)
7. 1000uM Fe(II)
8. 1000uM Fe(II)
Chl (ug/ml)
Time(hr)

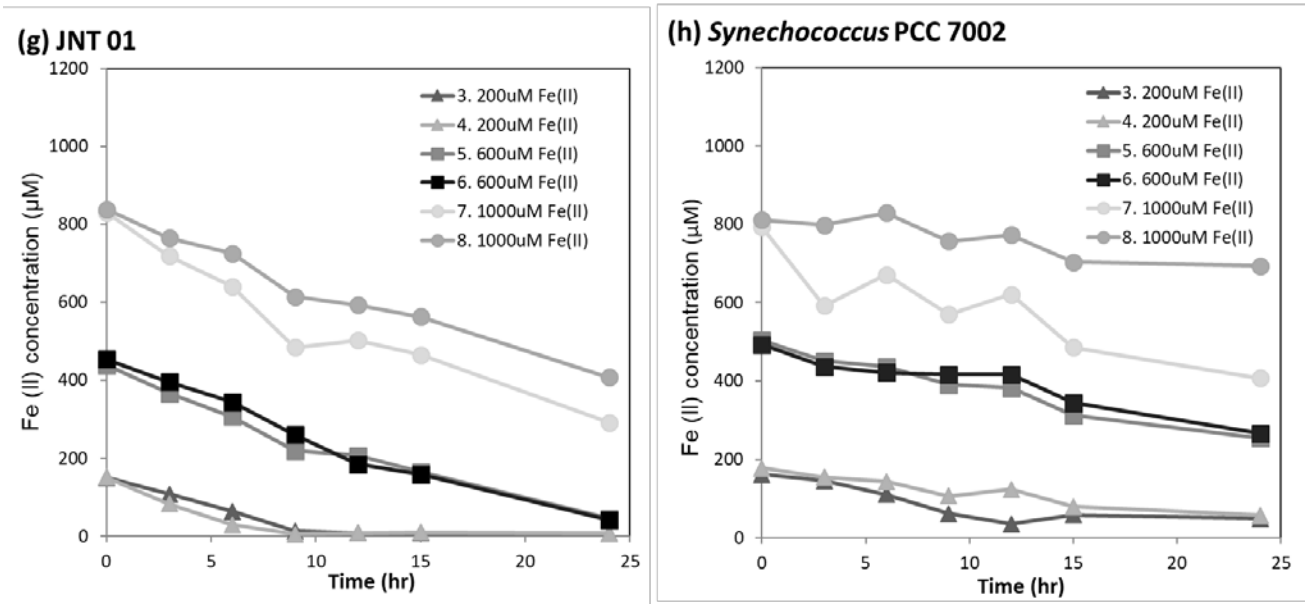

Fig. 11 Growth of JNT01 and *Synechococcus* PCC 7002 and Fe(II) concentration at different Fe(II) concentration. Initial cyanobacterial concentration inoculated was 0.05 μg/ml chlorophyll. Ferric ammonium citrate was not added. (a) JNT01 growth curve, (b) close up (a), (c) the data from (a) were plotted on a log scaled axis. (d) *Synechococcus* PCC 7002 growth curve, (e) close up (d), (f) the data from (d) were plotted on a log scaled axis. (g) Fe(II) measurements from representative replicates of experiments where JNT 01 was grown under conditions that began anoxic with 200 μM (triangles), 600 μM (squares) 1000 μM(circles), initial Fe(II). (h) Fe(II) measurements of *Synechococcus* PCC 7002.

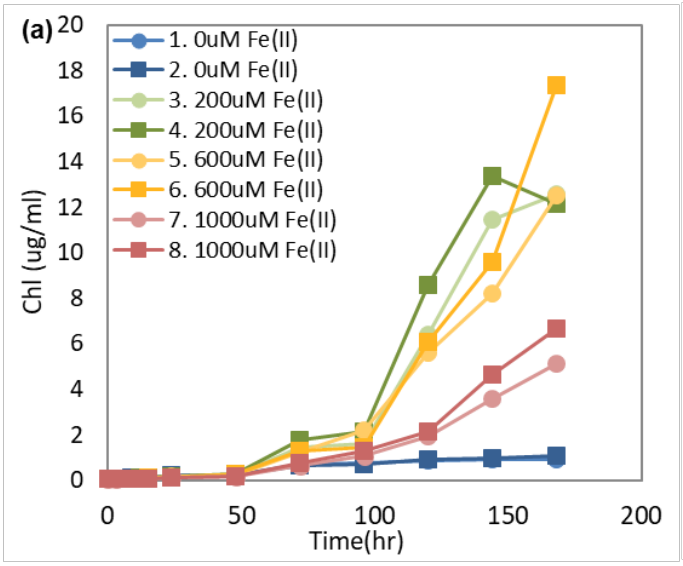
(a)
1. 0uM Fe(II)
2. 0uM Fe(II)
3. 200uM Fe(II)
4. 200uM Fe(II)
5. 600uM Fe(II)
6. 600uM Fe(II)
7. 1000uM Fe(II)
8. 1000uM Fe(II)
Chl (ug/ml)
Time(hr)

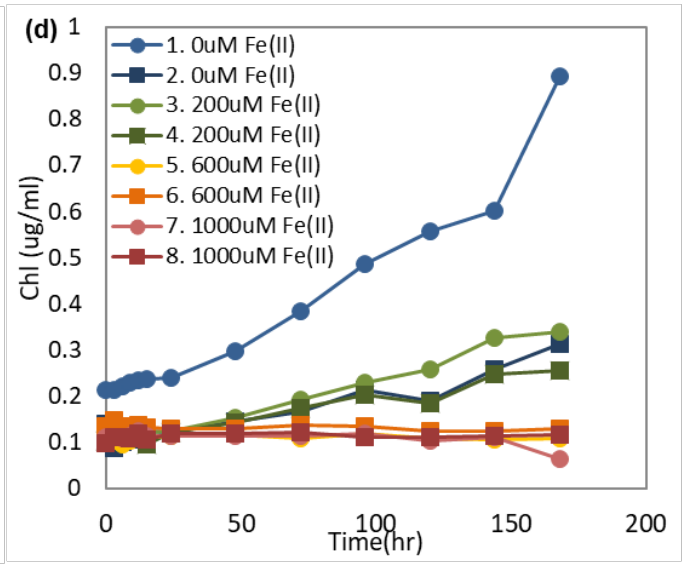
(d)
1. 0uM Fe(II)
2. 0uM Fe(II)
3. 200uM Fe(II)
4. 200uM Fe(II)
5. 600uM Fe(II)
6. 600uM Fe(II)
7. 1000uM Fe(II)
8. 1000uM Fe(II)
Chl (ug/ml)
Time(hr)

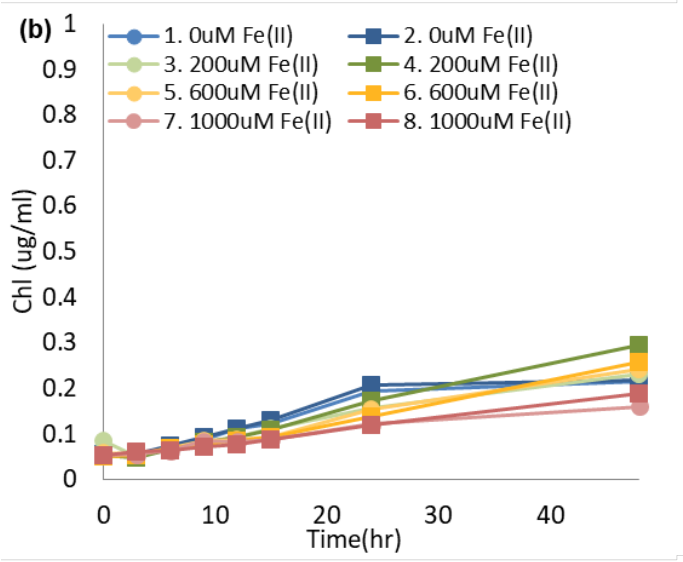
(b)
1. 0uM Fe(II)
2. 0uM Fe(II)
3. 200uM Fe(II)
4. 200uM Fe(II)
5. 600uM Fe(II)
6. 600uM Fe(II)
7. 1000uM Fe(II)
8. 1000uM Fe(II)
Chl (ug/ml)
Time(hr)

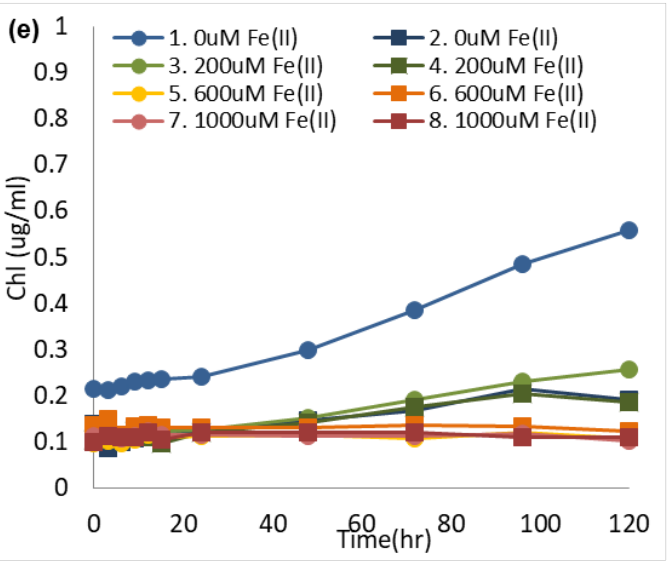
(e)
1. 0uM Fe(II)
2. 0uM Fe(II)
3. 200uM Fe(II)
4. 200uM Fe(II)
5. 600uM Fe(II)
6. 600uM Fe(II)
7. 1000uM Fe(II)
8. 1000uM Fe(II)
Chl (ug/ml)
Time(hr)

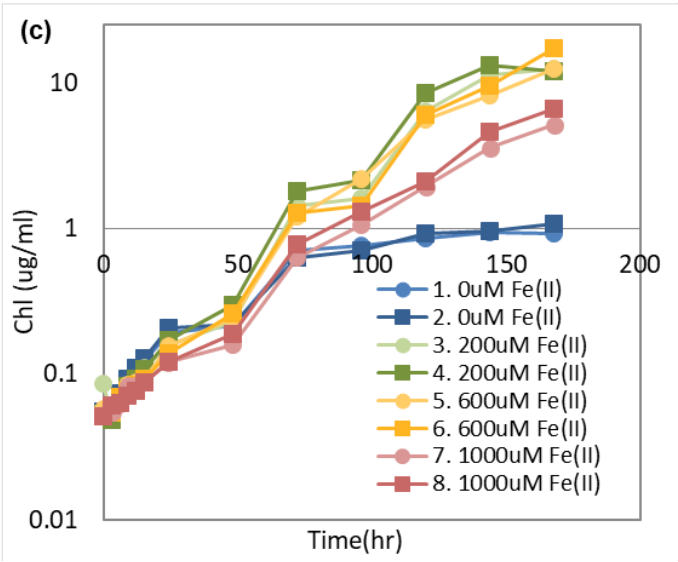
(c)
1. 0uM Fe(II)
2. 0uM Fe(II)
3. 200uM Fe(II)
4. 200uM Fe(II)
5. 600uM Fe(II)
6. 600uM Fe(II)
7. 1000uM Fe(II)
8. 1000uM Fe(II)
Chl (ug/ml)
Time(hr)

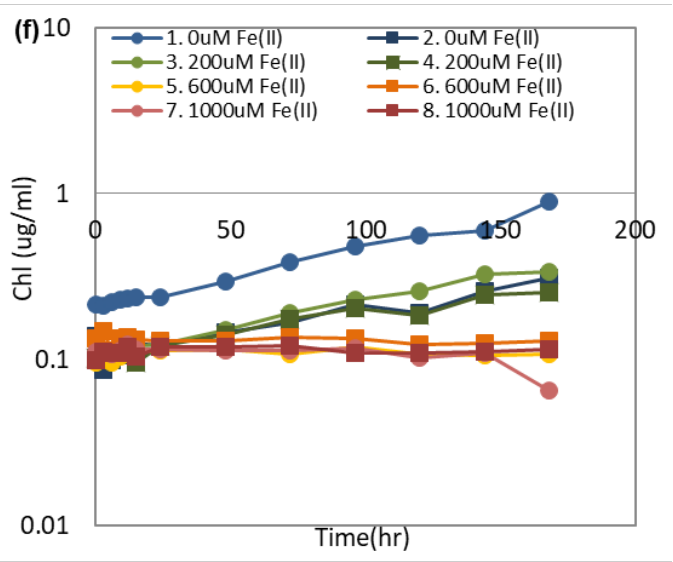
(f)
1. 0uM Fe(II)
2. 0uM Fe(II)
3. 200uM Fe(II)
4. 200uM Fe(II)
5. 600uM Fe(II)
6. 600uM Fe(II)
7. 1000uM Fe(II)
8. 1000uM Fe(II)
Chl (ug/ml)
Time(hr)

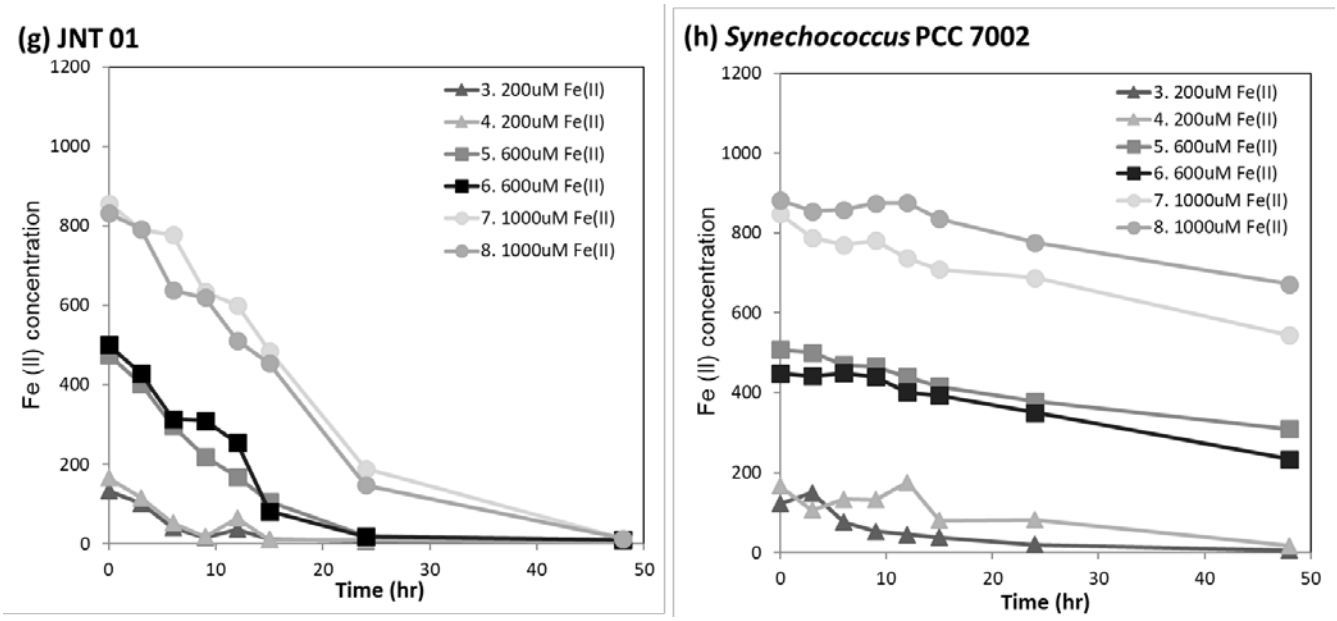

Fig. 12 Growth of JNT01 and *Synechococcus* PCC 7002 and Fe(II) concentration at different Fe(II) concentration. Initial cyanobacterial concentration inoculated was 0.05 µg/ml chlorophyll. Ferric ammonium citrate was not added. Experimental conditions were the same as in Fig. 11. (a) JNT01 growth curve, (b) close up (a), (c) the data from (a) were plotted on a log scaled axis. (d) *Synechococcus* PCC 7002 growth curve, (e) close up (d), (f) the data from (d) were plotted on a log scaled axis. (g) Fe(II) measurements from representative replicates of experiments where JNT 01 was grown under conditions that began anoxic with 200 µM (triangles), 600 µM (squares) 1000 µM(circles), initial Fe(II). (h) Fe(II) measurements of *Synechococcus* PCC 7002.

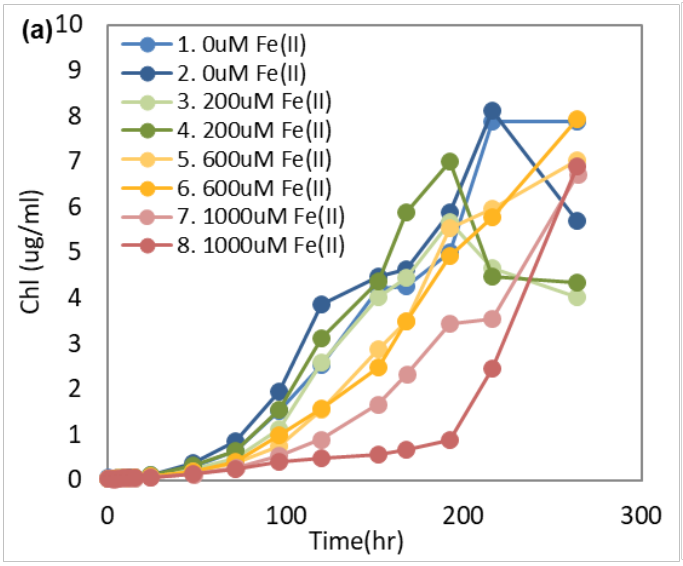
(a)
Chl (ug/ml)
Time(hr)
1. 0uM Fe(II)
2. 0uM Fe(II)
3. 200uM Fe(II)
4. 200uM Fe(II)
5. 600uM Fe(II)
6. 600uM Fe(II)
7. 1000uM Fe(II)
8. 1000uM Fe(II)

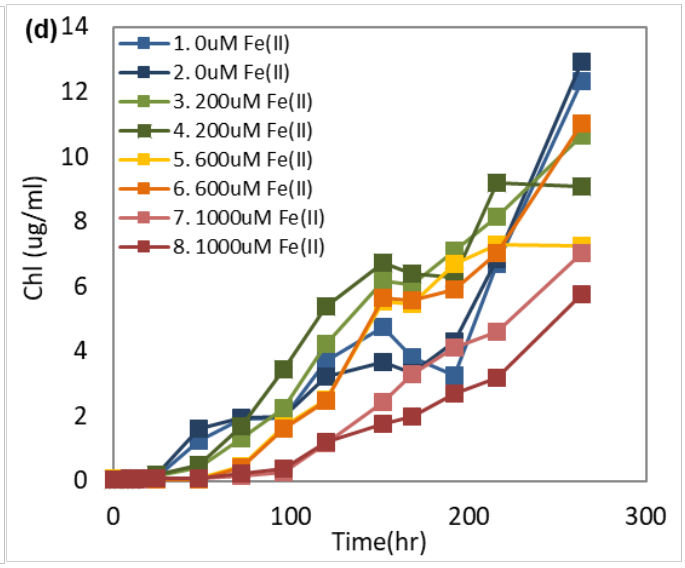
(d)
Chl (ug/ml)
Time(hr)
1. 0uM Fe(II)
2. 0uM Fe(II)
3. 200uM Fe(II)
4. 200uM Fe(II)
5. 600uM Fe(II)
6. 600uM Fe(II)
7. 1000uM Fe(II)
8. 1000uM Fe(II)

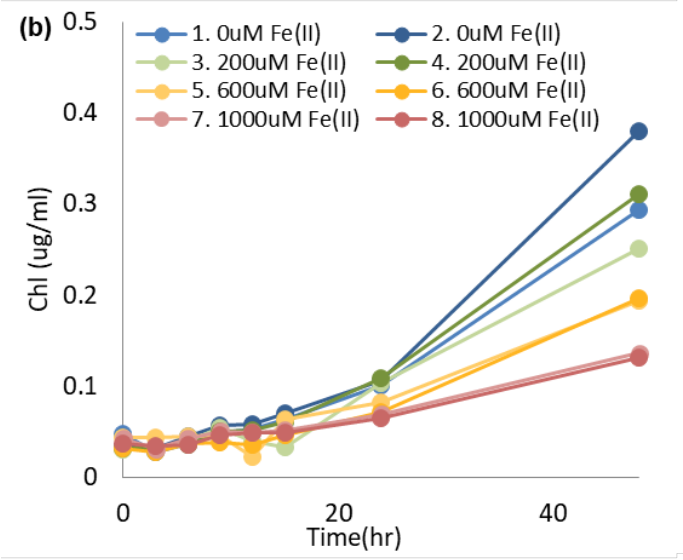
(b)
Chl (ug/ml)
Time(hr)
1. 0uM Fe(II)
2. 0uM Fe(II)
3. 200uM Fe(II)
4. 200uM Fe(II)
5. 600uM Fe(II)
6. 600uM Fe(II)
7. 1000uM Fe(II)
8. 1000uM Fe(II)

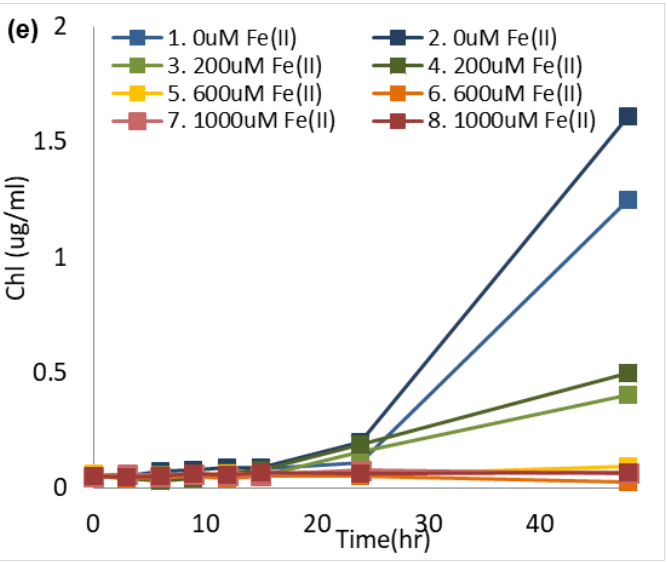
(e)
Chl (ug/ml)
Time(hr)
1. 0uM Fe(II)
2. 0uM Fe(II)
3. 200uM Fe(II)
4. 200uM Fe(II)
5. 600uM Fe(II)
6. 600uM Fe(II)
7. 1000uM Fe(II)
8. 1000uM Fe(II)

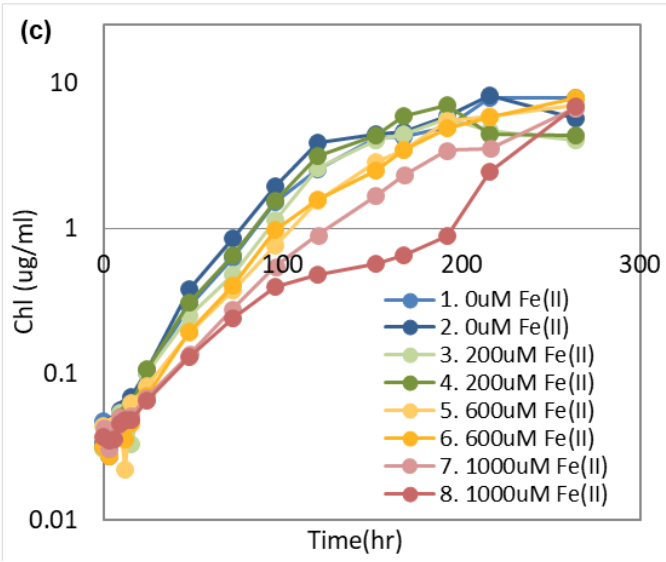
(c)
Chl (ug/ml)
Time(hr)
1. 0uM Fe(II)
2. 0uM Fe(II)
3. 200uM Fe(II)
4. 200uM Fe(II)
5. 600uM Fe(II)
6. 600uM Fe(II)
7. 1000uM Fe(II)
8. 1000uM Fe(II)

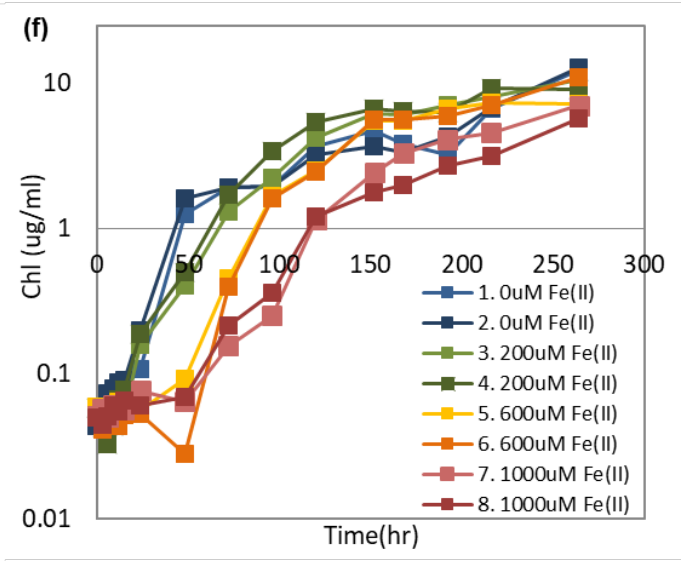
(f)
Chl (ug/ml)
Time(hr)
1. 0uM Fe(II)
2. 0uM Fe(II)
3. 200uM Fe(II)
4. 200uM Fe(II)
5. 600uM Fe(II)
6. 600uM Fe(II)
7. 1000uM Fe(II)
8. 1000uM Fe(II)

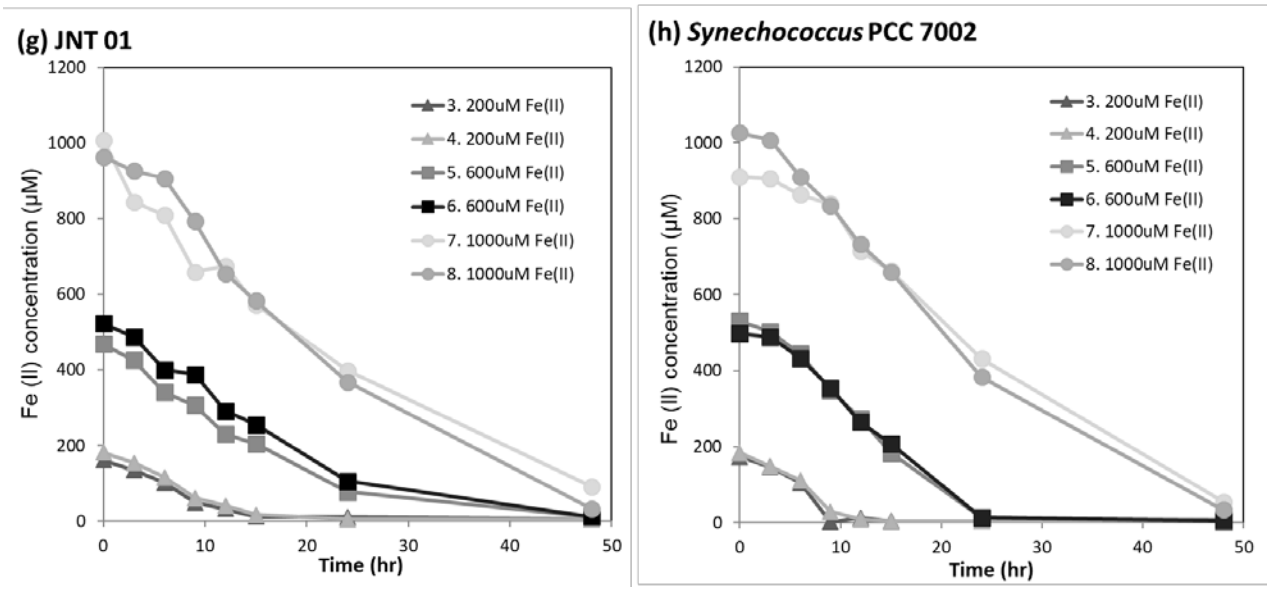

Fig. 13 Growth of JNT 01 and *Synechococcus* PCC 7002 and Fe(II) concentration at different Fe(II) concentration. Initial cyanobacterial concentration inoculated was 0.05 µg/ml chlorophyll. Ferric ammonium citrate was added after autoclaving.

(a) JNT 01 growth curve, (b) close up (a), (c) the data from (a) were plotted on a log scaled axis. (d) *Synechococcus* PCC 7002 growth curve, (e) close up (d), (f) the data from (d) were plotted on a log scaled axis. (g) Fe(II) measurements from representative replicates of experiments where JNT 01 was grown under conditions that began anoxic with 200 µM (triangles), 600 µM (squares) 1000 µM(circles). (h) Fe(II) measurements of *Synechococcus* PCC 7002.

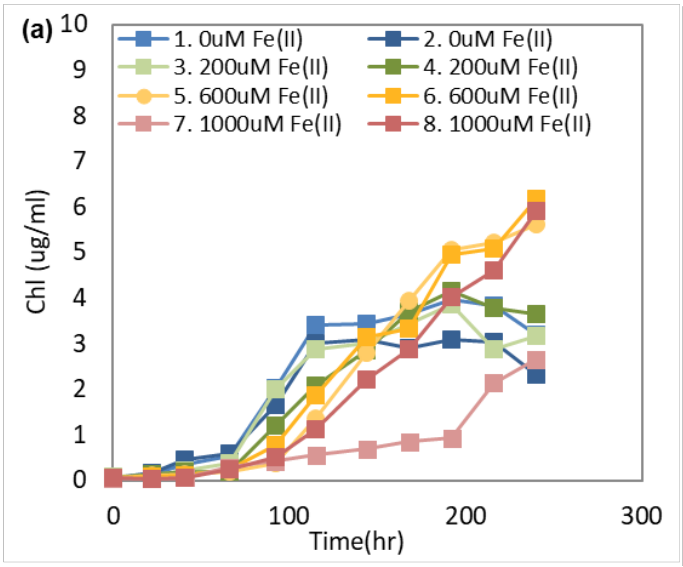
(a)
1. 0uM Fe(II)
2. 0uM Fe(II)
3. 200uM Fe(II)
4. 200uM Fe(II)
5. 600uM Fe(II)
6. 600uM Fe(II)
7. 1000uM Fe(II)
8. 1000uM Fe(II)
Chl (ug/ml)
Time(hr)

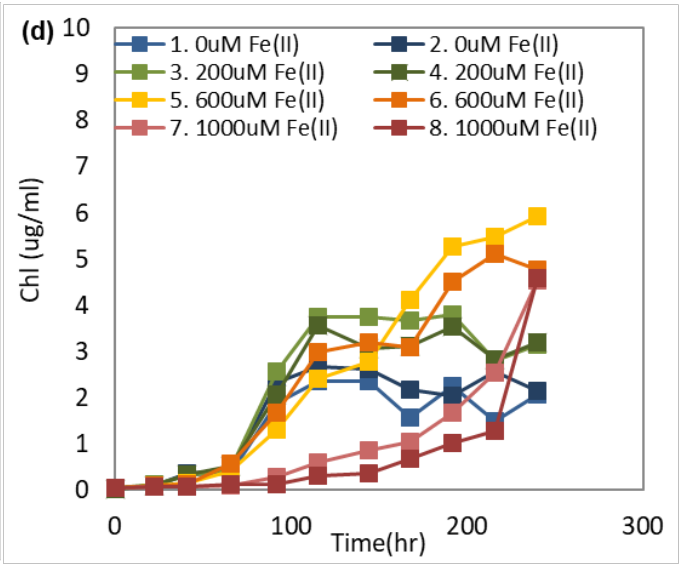
(d)
1. 0uM Fe(II)
2. 0uM Fe(II)
3. 200uM Fe(II)
4. 200uM Fe(II)
5. 600uM Fe(II)
6. 600uM Fe(II)
7. 1000uM Fe(II)
8. 1000uM Fe(II)
Chl (ug/ml)
Time(hr)

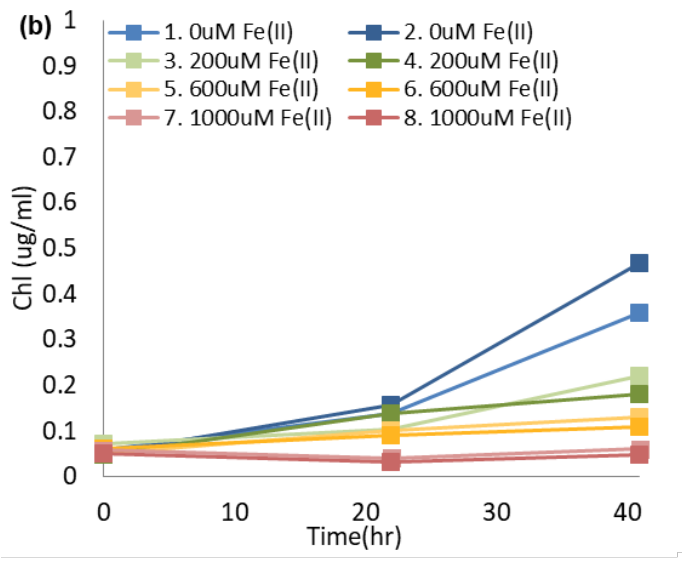
(b)
1. 0uM Fe(II)
2. 0uM Fe(II)
3. 200uM Fe(II)
4. 200uM Fe(II)
5. 600uM Fe(II)
6. 600uM Fe(II)
7. 1000uM Fe(II)
8. 1000uM Fe(II)
Chl (ug/ml)
Time(hr)

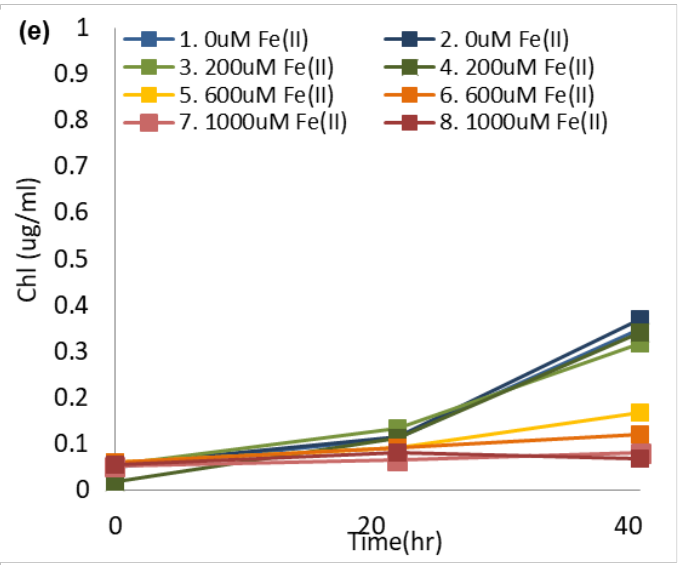
(e)
1. 0uM Fe(II)
2. 0uM Fe(II)
3. 200uM Fe(II)
4. 200uM Fe(II)
5. 600uM Fe(II)
6. 600uM Fe(II)
7. 1000uM Fe(II)
8. 1000uM Fe(II)
Chl (ug/ml)
Time(hr)

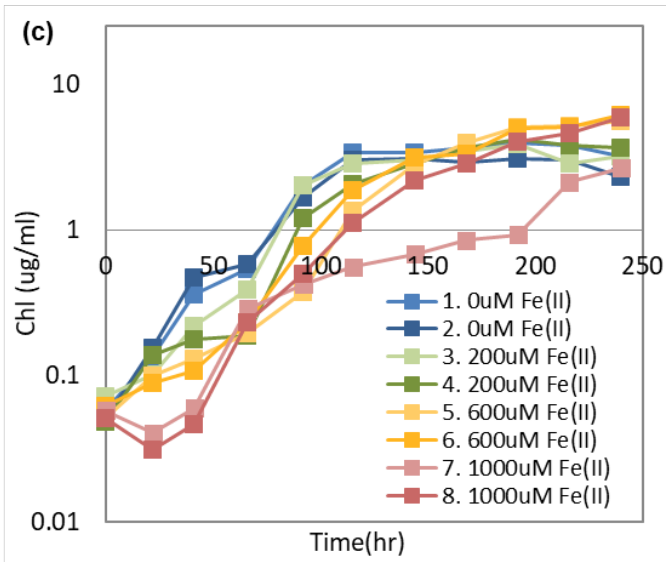
(c)
1. 0uM Fe(II)
2. 0uM Fe(II)
3. 200uM Fe(II)
4. 200uM Fe(II)
5. 600uM Fe(II)
6. 600uM Fe(II)
7. 1000uM Fe(II)
8. 1000uM Fe(II)
Chl (ug/ml)
Time(hr)

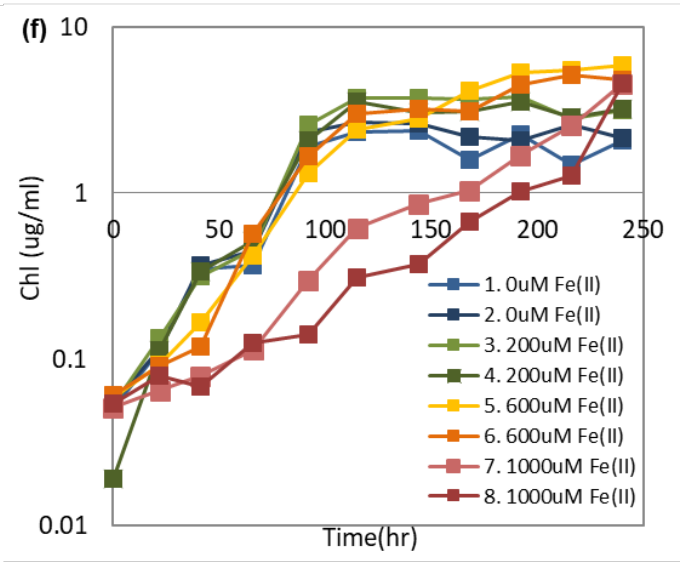
(f)
1. 0uM Fe(II)
2. 0uM Fe(II)
3. 200uM Fe(II)
4. 200uM Fe(II)
5. 600uM Fe(II)
6. 600uM Fe(II)
7. 1000uM Fe(II)
8. 1000uM Fe(II)
Chl (ug/ml)
Time(hr)

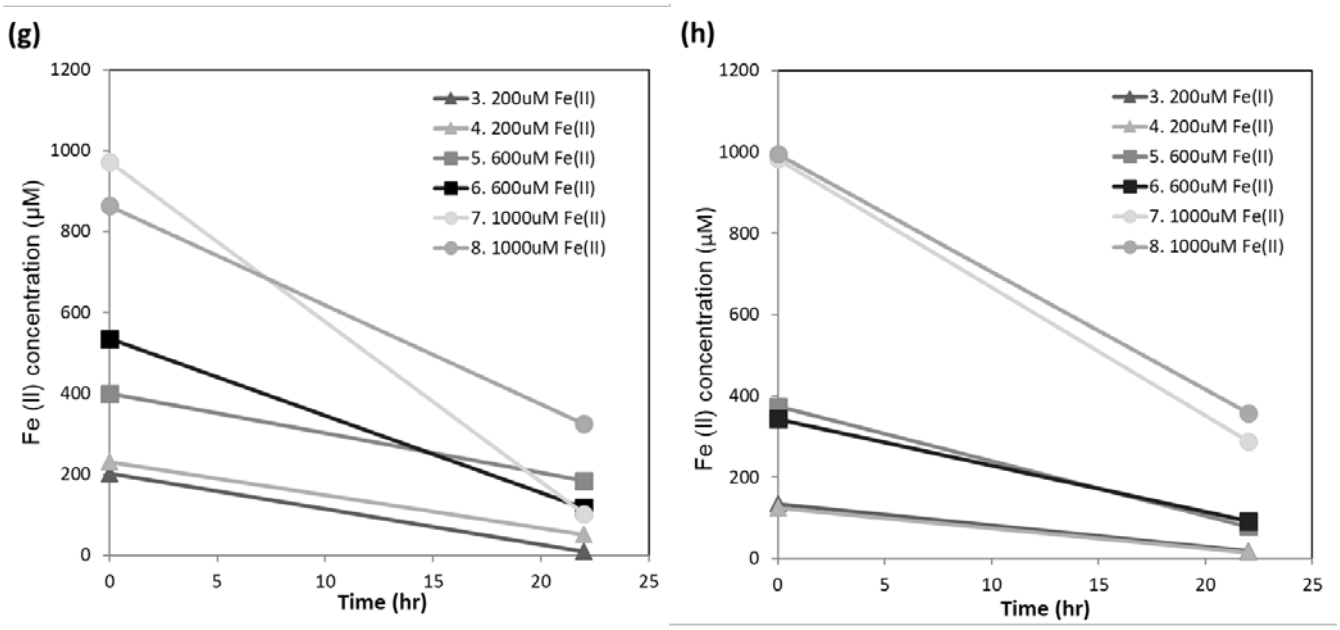

Fig. 14. Growth of *Synechococcus* PCC 7002 (pH 8.5 and pH 7.5) and Fe(II) concentration at different Fe(II) concentration. Initial cyanobacterial concentration inoculated was 0.05 µg/ml chlorophyll. Ferric ammonium citrate was added after autoclaving. Experimental conditions were the same as in Fig. 11 except pH (the normal pH in other experiments was 7.5)

(a) *Synechococcus* PCC 7002 growth curve (pH 8.5), (b) close up (a), (c) the data from (a) were plotted on a log scaled axis. (d) *Synechococcus* PCC 7002 growth curve (pH 7.5), (e) close up (d), (f) the data from (d) were plotted on a log scaled axis. (g) Fe(II) measurements from representative replicates of experiments where JNT 01 was grown under conditions that began anoxic with 200 µM (triangles), 600 µM (squares) 1000 µM(circles), initial Fe(II). (h) Fe(II) measurements of *Synechococcus* PCC 7002.

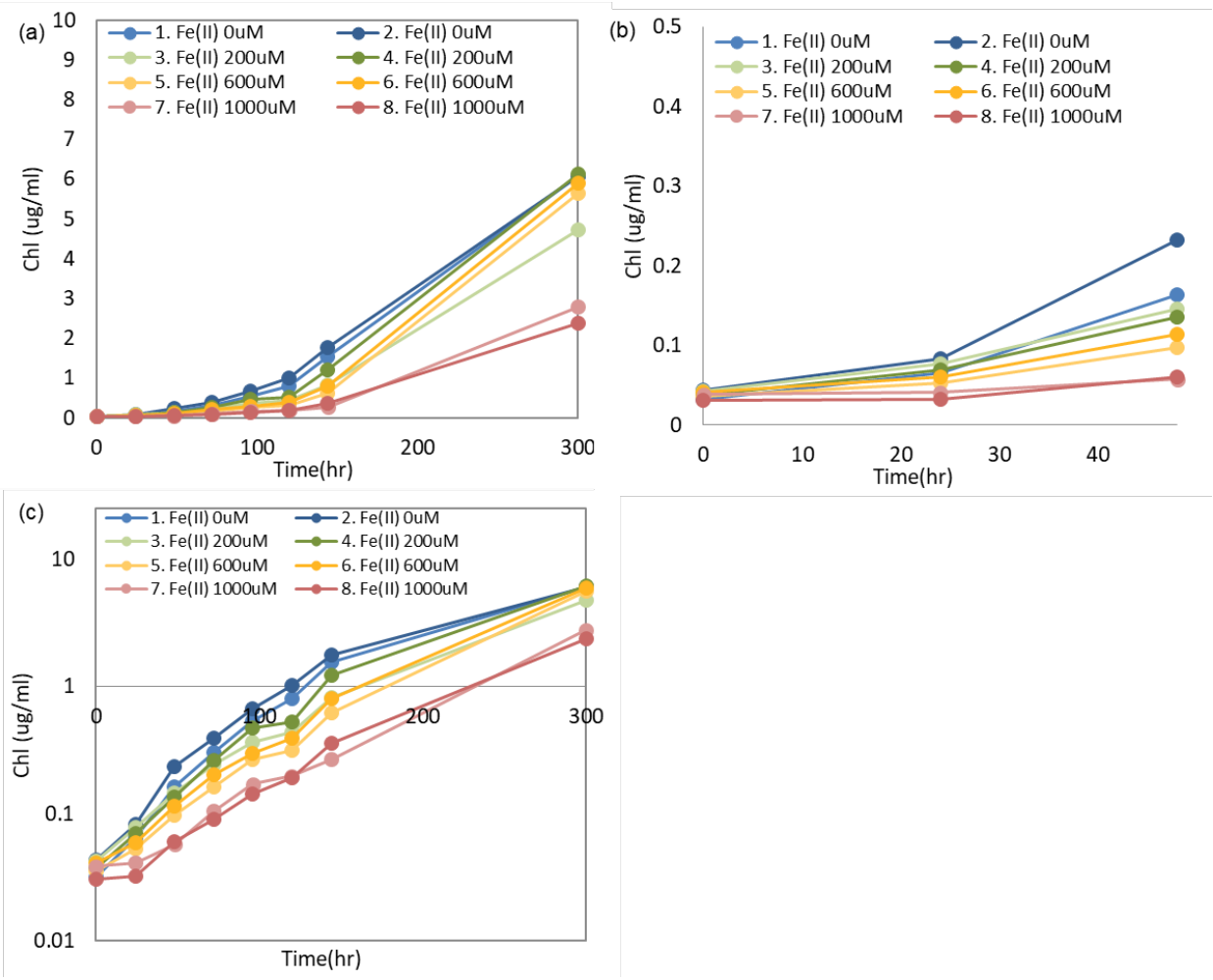

Fig. 15 Growth of JNT 01 at different Fe(II) concentration. Initial cyanobacterial concentration inoculated was 0.05 µg/ml chlorophyll. Ferric ammonium citrate was added after autoclaving.

Experimental conditions were the same as in Fig. 13. (a) JNT 01 growth curve, (b) close up (a), (c) the data from (a) were plotted on a log scaled axis.

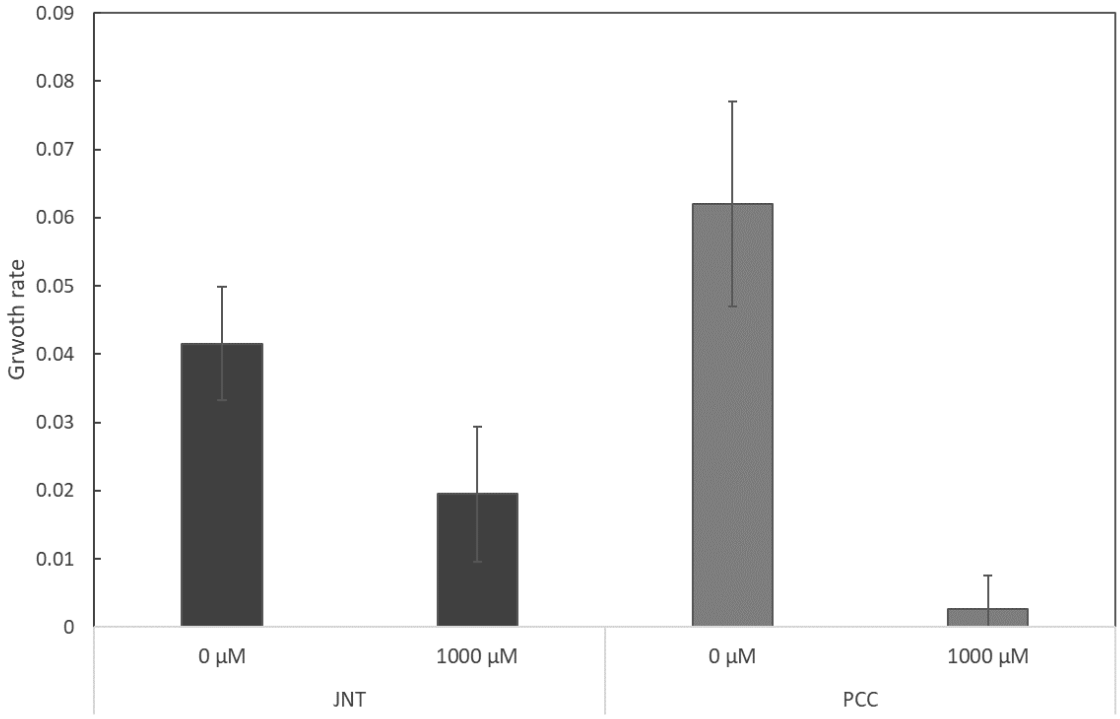

Fig. 16 Comparison of growth rate in the cultures of JNT 01 and PCC 7002 between 0 and 48 hours. Averages of Growth rates of between 0 and 48 hours in the cultures of the strains with 0 µM and 1000 µM Fe (II) n=4.

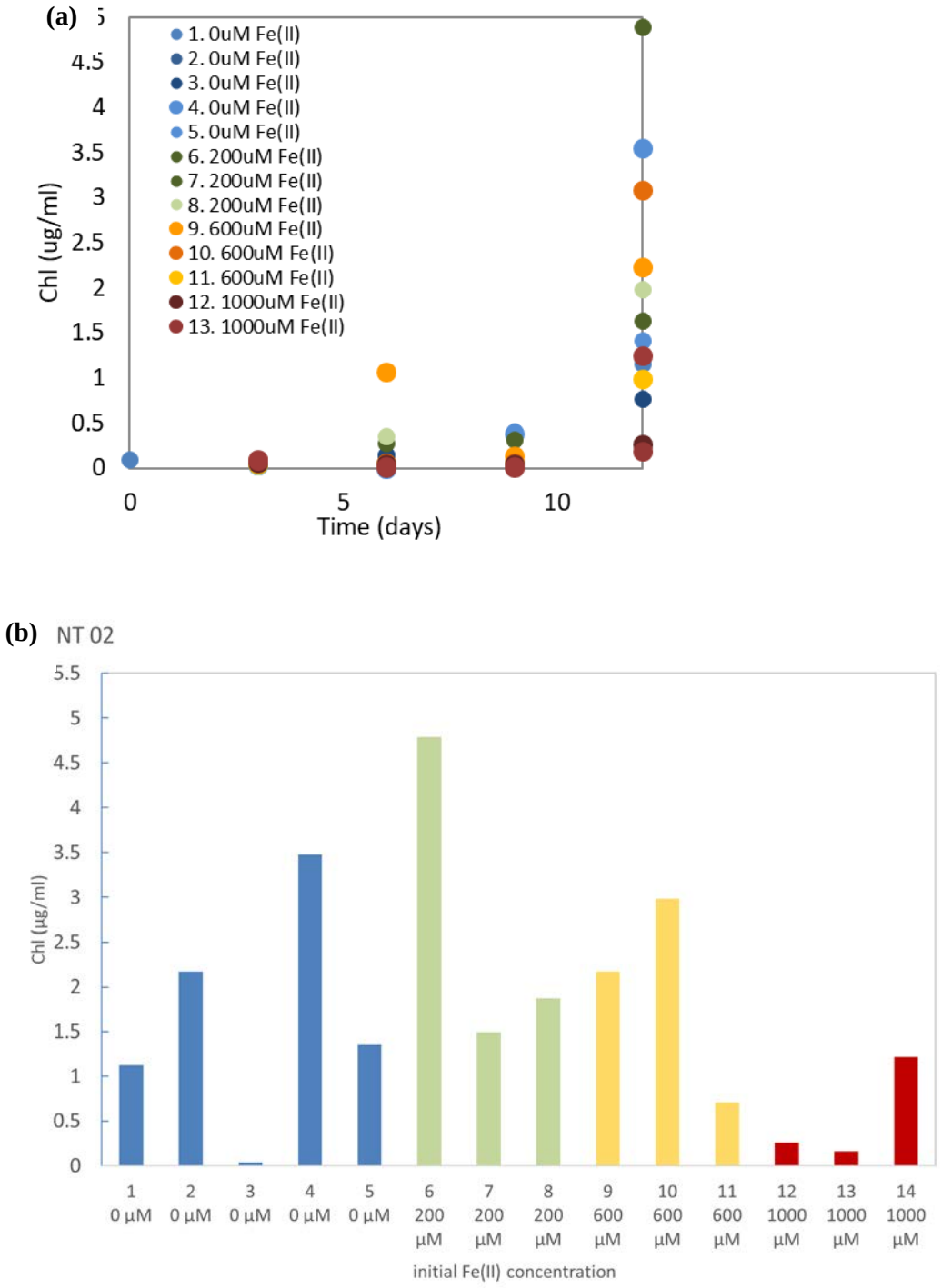

Fig. 17 Growth of JNT 02 at different Fe(II) concentration. Initial cyanobacterial concentration inoculated was 0.05 µg/ml chlorophyll. (a) show Chl concentrations of the cultures of JNT 02 in each day. (b) show Chl concentrations of the cultures of JNT 02 after 13 days.